Chapter 7

Observations of the Orionids meteor shower with the Buckland Park MF radar

The optimised radar system was used to observe numerous meteor shower and sporadic events over a two and a half year period. Preliminary examination of these observations reveals a significant variation in the quantity and quality of meteor echoes detected. This situation is a direct consequence of the necessary experimentation in radar collection parameters to optimise meteor observations at 2 MHz (e.g. PRF, time series length, transmit beam configuration etc.), the effects of ionospheric phenomena (e.g. echo masking due to layering, absorption due to D-region etc.) and variability of the meteor events themselves (e.g. activity etc.). Observations conducted on the peak night of the Orionids shower, 22 October 2000, were determined to be of significantly better quality than the average, while displaying typical shower echo rates, and it is these results that are presented and discussed in this Chapter.

We begin this discussion with a brief summary of the scientific research into the Orionid meteor shower as it pertains to this current work. This is followed by an estimate of the Orionid meteor component contribution to the total observed meteor events, obtained using the coordinate transform technique of *Elford* [1954] as detailed

earlier (see section 6.3.4). Further analysis of this selected component follows.

7.1   Previous Orionids meteor shower research

The Orionids (October) and η-Aquarids (May) meteor showers have long known to be associated with Comet 1P/Halley due to their orbits having similar inclinations, longitudes of perihelion and perihelion distances [*McKinley*, 1961; *Jones*, 1983] and it is certain that these two distinct showers are caused by the passage of the Earth through the parent comet's debris before and after perihelion [*Lovell*, 1954]. This association has been confirmed, for instance, with the stream modelling of *Hajduk* [1970] and *McIntosh & Hajduk* [1983], based on observations extending back to 1900 AD and 1404 BC respectively.

Lovell [1954] summarises the visual, camera and early radar observations of the Orionids conducted early to mid last century, and notes an observed non-stationary behaviour of the radiant attributed to the Earth's passage through filamentary structures of the stream. This apparent "movement" of the radiant of the Orionids shower has been re-investigated over the ensuing years and a brief summary of the early debate of the structure of the Orionids is outlined by *Lindblad & Porubcan* [1999]. Early attempts at velocity measurements using photographic and visual techniques [*Millman & Hoffleit*, 1937; *Porter*, 1943] did not provide conclusive characteristic mean speeds for this shower. More accurate speeds were first derived from double-camera data [*Jacchia*, 1948] and are given as 66.58 and 65.28 km s^{-1} for the shower observations in 1939 and 1946 respectively.

Modern visual, telescopic, photographic and video research (1945 to 1995) of the Orionids has been summarised by *Lindblad & Porubcan* [1999]. Here we will concentrate on the radar investigations applicable to this study. The first determinations of Orionid radiant positions and hourly rates from radio echo observations were published by *Hawkins & Almond* [1952]. Their results, and those of most researchers discussed in the following paragraphs are tabulated in Table 7.1. The first radar observations of this

shower at Adelaide (and in the southern hemisphere), were made by *Weiss* [1955] who determined a peak activity of 20 meteors per hour on 25 October 1952, but published no radiant result. This researcher also noted that no shower was detected during 1953. The Orionids shower was present in the southern hemisphere radio survey of *Nilsson* [1964], also from an Adelaide site. Employing a combination CW and pulse radar operating at 27 MHz, meteoroid velocity was determined using spatially separated receive sites and the diffraction maxima and minima of the echo. Other non-Orionid meteors that occurred within the acknowledged activity period of the Orionids were also recorded. These had lower mean speeds of 22-35 km s^{-1}. *Kashcheyev & Lebedinets* [1967] summarise radar meteor observations in terms of meteoroid streams and compare their results with that of other researchers. In this particular study the meteoroid speed was determined by the pulse diffraction method of *Ellyett & Davies* [1948].

A series of papers [*Hajduk*, 1970; *Hajduk*, 1973; *Hajduk*, 1980], including some radar data from Ottawa (Canada) and Ondřejov (Czech Republic) sites, investigated the Comet Halley stream structure via the η-Aquarids and Orionids showers; the total mass of the stream was determined by *Hajduk* [1982].

Gartrell & Elford [1975], using a 27 MHz radar at an Adelaide site, also detected the Orionid stream amongst others in their comprehensive southern hemisphere survey. Results were compared to other surveys with generally good agreement. Interestingly, in relation to the October observations encompassing the Orionids activity, some meteors were found to have velocities exceeding 74 km s^{-1}. They suggest that "strongly hyperbolic meteors observed at Earth may be the result of recent perturbations and need not imply interstellar origins". Another example exhibits a speed of 71 km s^{-1} and hyperbolic orbital elements in agreement with another researcher [*Lindblad*, 1971].

Sekanina [1976] reported on data from the Radio Meteor Project at Havana, Illinois, collected during 1961 to 1965, where orbital parameters were determined for the Orionids, including meteoroid speeds. Data from 1968 to 1969 was also employed, and a significant number of additional October showers listed.

Using a 40.358 MHz radar operated during 1980 and 1981, *Jones* [1983] focused on

radiant activity and position over consecutive days, absolute particle flux and mass distribution of the Orionids. In terms of the radiant position, he found large fluctuations in declination from day to day, but noted this may be a real or possibly instrumental effect. If the effect is real, he suggested that it could be the result of transient bursts of activity from filaments within the total stream.

A recent study of this stream by *Lindblad & Porubcan* [1999] using photographic data of "bright" meteors (i.e. relatively large meteoroids) available from the IAU Meteor Data Center observed over a period from 1936 to 1993, showed that the previously reported complicated radiant structure is not present in the archived data. Video data was also examined with a similar result.

It should be noted that four of the last five radiant studies cited in Table 7.1 determine the radiant (α, δ) to be $(95°,16°)$. This is the radiant coordinate chosen for determining the beam position of the BP 2 MHz radar for optimum data rate (see Table 6.2 on page 295). It was also the coordinate used for the selection of Orionid shower meteors from the 2 MHz radar data as discussed below.

Authors	Method	α [°]	δ [°]	V [km s^{-1}]	N
Hawkins & Almond [1952]	radar	95	13	-	82
		98	9	-	70
Nilsson [1964]	radar	96.7	14.4	65.3	6
Kashcheyev & Lebedinets [1967]	radar	93	16	66	61
Gartrell & Elford [1975]	radar	94	14	67	6
Sekanina [1976]	radar	94.6	16.1	65.3	17
Jones [1983]	radar	94.15	15.47	-	342
Jenniskens [1994]	visual	95	16	67	2428
McBeath & Arlt [2000]	-	95	16	66	-
Lindblad & Porubcan [1999]	photographic	94.64	15.79	-	60

Table 7.1: Orionids shower characteristics. A selection of primarily radar derived shower characteristics of right ascension (α), declination (δ), velocity (V) and number of contributing meteors (N). The last three entries are comprehensive, primarily non-radar studies for comparison. A radiant (α,δ) of ($95°,16°$) was employed in radar beam direction calculations and meteor shower selection.

Jones et al. [1989] re-visited the Ontario (40.358 MHz) [*Jones*, 1983], Ottawa

(32.7 MHz) and Ondrejov (37.5MHz) [*Hajduk*, 1982] radar data, as well as TV and visual data in order to determine the age of the Orionid meteoroid stream. Their age of 2.3×10^4 years is in general agreement with other age determinations.

Although not a study of the Orionid shower as such, *Tsutsumi et al.* [1999] used the Buckland Park radar system for meteor wind observations that incidentally occurred during the Orionids shower of 22 October 1997. They reported on the contribution of underdense Orionids meteors to the total detected during the viewing time and estimated that such a contribution was no greater than 40%. This was determined via the application of a great circle transform technique [*Poole & Roux*, 1989].

7.2 Radiant selection using reflection point geometry

In order to identify radar meteor echoes that are associated with a particular shower radiant two procedures have been developed [*Elford*, 1954; *Jones & Morton*, 1977]. In both cases the observations are transformed from the observer's frame of reference to one based on celestial coordinates. The procedure used in what follows is based on *Elford* [1954] and has already been described in section 6.3.4. In summary, the radar meteor reflection point data is transformed from azimuth angle, zenith angle and local time (after midnight) coordinates (ϕ_A, θ_A, t) in the radar observer's reference frame to polar coordinates $(\tan \alpha, T = \phi + \frac{t}{4})$ in the celestial frame in order to identify source radiants. In the latter frame, α is the angle the reflection point vector makes with the celestial polar axis and ϕ is the angle measured eastwards from transit to the projection of the reflection point vector on the celestial equatorial plane (see Figure 6.14 on page 343). This polar plot representation allows echoes from a source radiant to lie on a straight line defined by the hour angle (H) and declination (δ) as described in Figure 6.16 on page 345.

Figure 7.1 displays the result of this transformation for the data of 22 October 2000 over the period 00:00 to 05:40 LT. A small number of echoes resulting in an ambiguous angle-of-arrival (AoA) were excluded from the data set. A total of 108 echoes, from
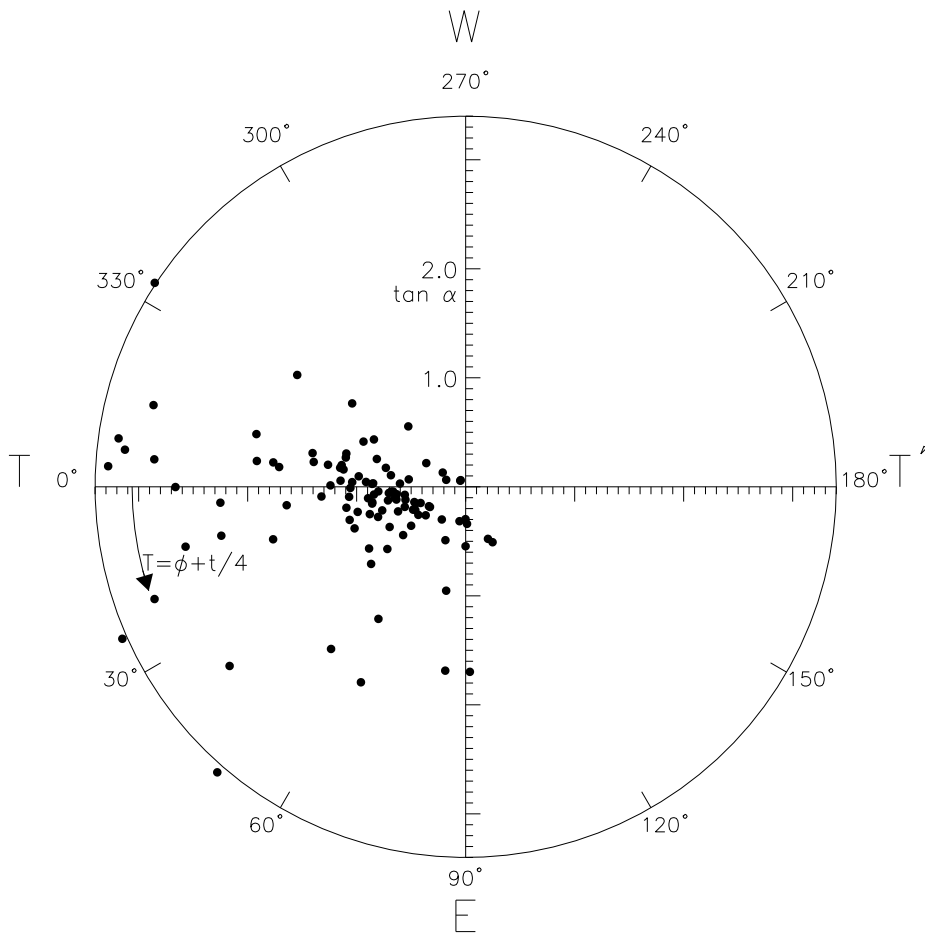
Figure 7.1: Reflection point data (ϕ_A, θ_A, t) of 22 October 2000 transformed to the celestial frame ($|\tan\alpha|$, $T = \phi + \frac{t}{4}$). Number of echoes $(N) = 108$.

which all necessary parameters were reduced, are included here. Note that $|\tan\alpha|$ has been limited to the range $0 \le |\tan\alpha| \le 3.4$ in order to adequately display the main features. A similar approach of varying the extent of the radial axis is taken in subsequent plots and it thus should be understood that a small number of meteor echoes exist at greater values of $|\tan\alpha|$ than is plotted. While these echoes are not displayed for the sake of overall clarity of the majority of echoes being studied near the centre of this figure, they are however included in the analysis where necessary.

In accessing the figure's general features we observe that all echoes are confined to the first ($0° \le \phi \le 90°$), second ($90° \le \phi \le 180°$) and fourth ($270° \le \phi \le 360°$) quadrants. This is the result of a number of factors (e.g. radar response function, active

shower etc.) and these will be discussed in turn later. Most significantly this general form is expected because observations from a particular geographical site allows certain regions of the celestial sphere to be clearly viewed while partially or totally obscurring other directions (i.e. a southern hemisphere site will better view the southern celestial hemisphere and view significantly less of the northern celestial hemisphere). This translates into less scatter across all quadrants of the diagram and promotes some partial clustering as observed here. This partial clustering is also apparent in a similar radar study of the 1952 Geminids [*Elford*, 1954, Figure 49]. In contrast to this, significant scatter is apparent in the simulated data of *Jones & Morton* [1977, Figure 5], indicating that site geography was not included in the model. The following sections address specific features identified in Figure 7.1.

7.3 Orionids primary component

As the Orionids is a major shower known to be active during October, the data presented were collected on the day of peak activity predicted for this shower. Knowledge of this shower's right ascension and declination of (95°, 16°) (see Table 7.1) can be used to select the dominant structure in the diagram. A line (dashed) corresponding to this radiant is indicated in Figure 7.2.

Because of the congested nature of the echoes in the region immediately surrounding this structure, radiant identification can be difficult. However in this case identification is aided by the presence of echoes occuring in the early morning (i.e. at start of observation period, just as the radiant has risen locally) and late morning (i.e. at end of the observation period) which are located on the polar plot at the extremies of the line appropriate to the radiant. From this it is apparent that the Orionids radiant coordinates select the dominant linear structure well.

This structure will be referred to as the Orionids-Primary (Orionids-P) radiant in the following analysis. Errors in the radiant hour angle (ΔH) and declination ($\Delta \delta$) are indicated by the lines (solid) surrounding the radiant line (dashed). These serve the
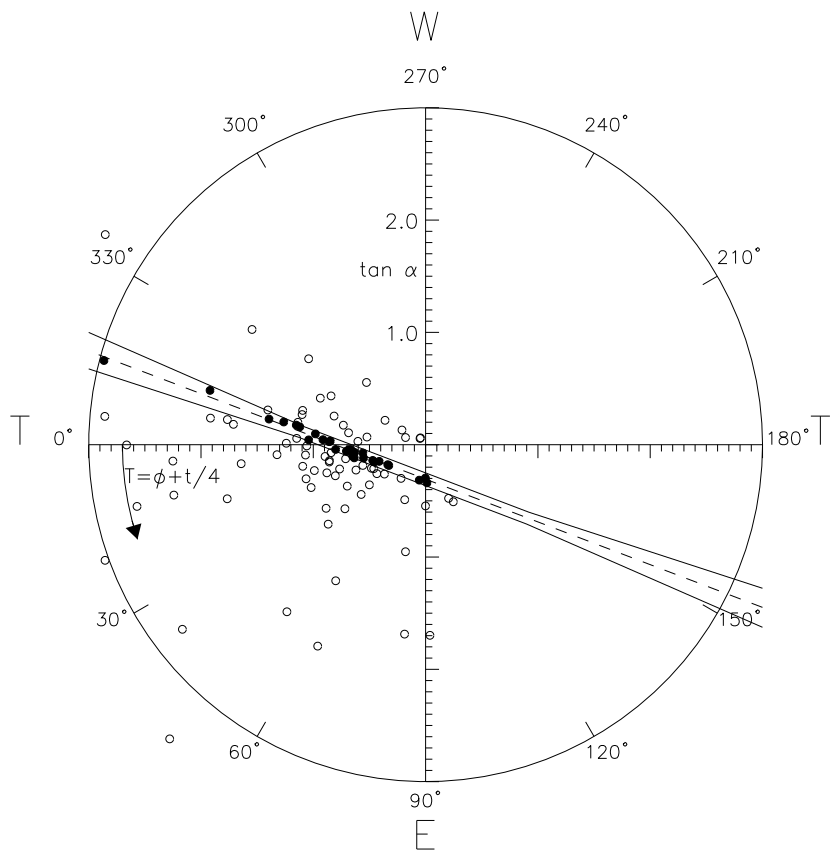
Figure 7.2: Celestial polar plot of 22 October 2000 meteor echoes including the Orionid radiant (95°, 16°) (dashed line) and radiant error (solid) $\Delta H, \Delta \delta = \pm 2.8°$. Thirty potential shower meteors (filled) are selected by this method.

dual purpose of encompassing any radiant variability and to aid in precise selection of meteors directly associated with a radiant of interest. Here $\Delta H, \Delta \delta = \pm 2.8°$ and the error in AoA is $\pm 3°$. Thirty potential meteors are selected as primary component shower meteors out of a total population of 108. The majority of these thirty meteors is expected to be from the Orionid radiant. From this figure it is also apparent that there exists a secondary linear structure immediately adjacent to, and aligned almost parallel with (i.e. similar hour angle), the selected primary radiant. This feature is discussed in section 7.4.

The population mix of a sample of meteors can be measured as a ratio (S) of shower to sporadic meteors (after *Jones & Morton* [1977]). Implementation of the transform technique (see Figure 7.2) has selected 30 potential Orionids-P meteors from a total sample of 108, thus $S = 30/(108 - 30) = 0.38$. It should be noted that this value

of thirty meteors is likely to include some sporadics at this stage of the analysis and therefore S should be interpreted as an approximation only. This measure can also be viewed as a shower strength index where S greater than unity is a strong shower and less than unity a weak shower. Alternatively a percentage of shower meteors $(30/108 = 28\%)$ to total observed meteors has been noted by others. In comparison to the mix found here, *Tsutsumi et al.* [1999] have by a similar analysis found that no more than 40% of underdense meteors were classed as Orionids for 22 October 1997. In any case the Orionids-P component is classified as a weak shower on the basis of the data presented here.

Assuming this polar plotting method selects "common" radiant meteors, other characteristics can be examined. Characteristics of particular importance are the meteor angle-of-arrival (AoA), height, speed, echo duration, etc. It is envisaged that the selected shower component will be a distinct sub-group of the total component across many of the characteristics examined, due to the distinct physical and atmospheric interaction characteristics that meteoroids from individual meteor streams possess.

7.3.1 Angle-of-arrival distribution

Having selected the Orionids-P radiant meteors after the echo data set is transformed, it is of interest to see where such echoes occur in the original radar observer's frame. The radar meteor echo reflection points from the radar observer's frame are displayed in Figure 7.3 (see section 6.3.4 for orientation details). The format of the plot is arranged such that concentric circles indicate $\sin(\text{zenith angle})$ for every $10°$ [*Nakamura et al.*, 1991; *Nakamura et al.*, 1997]. This allows more detail to be viewed around the region of interest than other angle-of-arrival representations, such that high off-zenith angle detail is suppressed in preference to mid-to-low off-zenith angle regions. Examining the sample in its entirety, most AoAs (both shower & non-shower) are observed from $150° \leq \phi_A \leq 315°$, i.e reflection points occur in the south-west sky. Within the total sample, the selected shower meteors are generally more tightly distributed about $170° \leq \phi_A \leq 255°$. This general clumping of both shower and non-shower
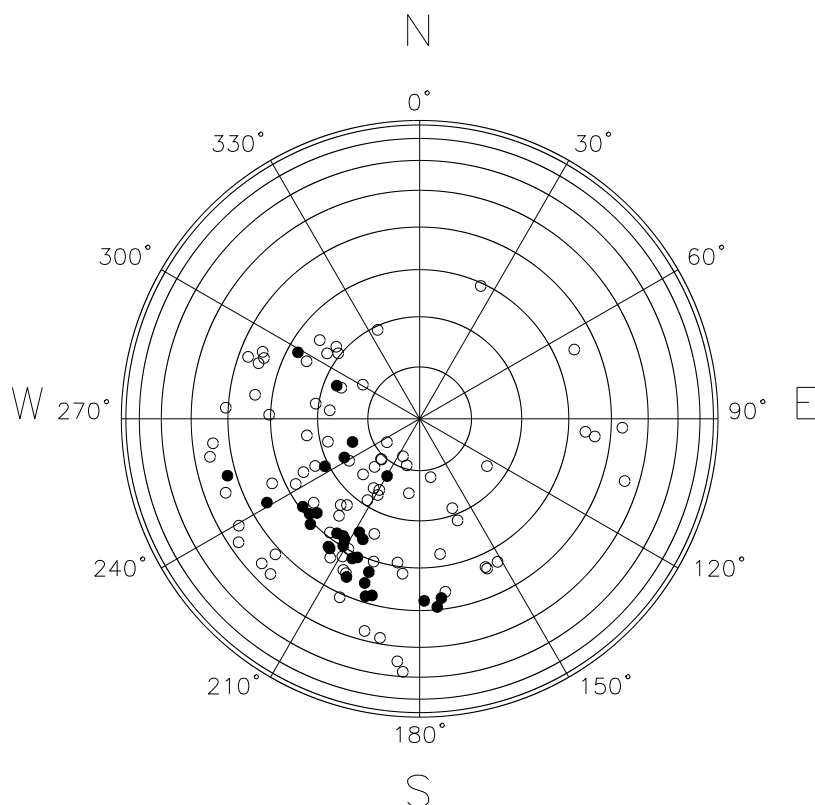
Figure 7.3: Meteor reflection point angle-of-arrival, 22 October 2000. Orionids-P (filled) echoes in comparison to total meteors detected (unfilled).

groups is expected. Sporadic meteoroid sources have been discussed previously (see section 5.2.1.1) with the helion source being dominant in this early morning observation period. Thus it is expected that most meteoroids will originate from the east with respect to the radar site. As the scattering mechanism responsible for most meteor echoes is a result of the trail forming perpendicular to the radar beam, most meteor reflection points will appear west of the radar. This is observed to be the case in Figure 7.3. The small number of non-shower or sporadic echoes detected in the eastern sky in this figure are likely due to bright meteors being detected in a minor lobe of the transmitted beam as it is steered to optimise the number of shower echoes. In addition to this, the general meteoroid complex observed on this day is augmented by the activity of the Orionids shower. The radiant position (azimuth & altitude), as

observed from the radar site, is given in Table 6.2 on page 295. This shows that the radiant position migrates in azimuth from near east (73°) anti-clockwise through north (342°) and rises to an altitude of 39° over the period of observation. It can be seen that the selected Orionid shower reflection points in Figure 7.3 are mostly contained within positions perpendicular to this radiant as expected.

Other features to note about the data indicated here is the low number of reflection points appearing near zenith. Most echoes are contained within zenith angles of 10° to 50°. This is to be expected considering meteoroid atmospheric entry geometry and transmitted beam geometry.

Although relatively few meteors are detected near the zenith, it has been noted previously [*Steel & Elford*, 1991] that data from Adelaide MF, HF and VHF radars, with their beam directed at small zenith angles ($z < 40°$, 2 MHz in this study; $z = 33.2°$ at 6 MHz; $z = 34°$ at 54.1 MHz), have more echoes at angles near zenith than typical meteor radars (i.e. $z \simeq 60 - 80°$ *Baggaley & Webb* [1980]). This has implications for the length and line density of the meteor trail produced, as meteoroids entering at shallow angles produce columns of ionisation which are longer and fainter [*Bronshten*, 1983].

The AoA result reported here is in good agreement with other reflection point distributions. *Tsutsumi et al.* [1999, Figure 8], using the Buckland Park MF radar, display AoA for underdense meteors for the morning of 22 October 1997. A similar clustering of reflection points away from the north-east was observed, as was a lack of echoes at near zenith. Again most echoes appeared between 25° to 50° zenith angles. It is assumed that a radiant distribution similar to that described for the October 2000 data was active in this case. The AoA distribution of *Nakamura et al.* [1991, Figure 6] from the MU radar displays a 24 hr observation period with few meteors detected at zenith angles less than 10°.

Recent theoretical modelling of the meteor echo sky distribution for the BP MF radar [*Cervera et al.*, 2003] is in agreement with the general form of Figure 7.3. The expected sky distribution due to four beam positions (24° zenith angle, directed at

azimuths of north, east, south and west) over the early morning observation period of 22 October 1997, was modelled and found to result in most echoes detected in the south-western quadrant of the sky.

7.3.2   Hourly rates

As the Orionid radiant rises at ∼23:20 LT and ground level sunrise is about 06:00 LT, the observation time nominally extended from 23:00 to 06:00 LT. However, few useable meteor echoes were observed in the first hour of observation and so the data presented here uses echoes observed from midnight local time. The end of this nominal observation period encompasses a dramatic increase in ionospheric layer production due to the rising sun and also required further scrutiny. It was over this latter period that a significant increase in "meteor echoes" was observed, with numerous "non-shower echoes" appearing at heights above 135 km. These anomalous echoes are likely to be due to contamination from the forming ionospheric layers (see e.g. *Steel & Elford* [1991]) and so were removed from the data set by terminating the observation period at 05:40 LT. This artifically reduces the number of echoes detected in the last hour of observation, which should be noted in the following discussion.

Figure 7.4 displays the total echo rate per hour (light shaded) in comparison to the selected (Orionids-P) shower meteors (dark shaded) over the period of observation. Local Time (LT) is Australian Central Standard Time (CST), which is 9 hrs 30 mins ahead of Universal Time (UT). In terms of the total echo rate per hour two features are significant. First, a maximum in echo rate is observed in the 2-3 LT period (35 echoes). This is followed by a sharp decline in echo rate and a observation period minimum (3 echoes) over 4-5 LT. The Orionids-P selected meteors (dark) display a echo rate maximum over the 2-3 LT period (15 echoes). A significant factor in the observed echo rate minimum at 4-5 LT is likely to be the reduced effectiveness of the transmitted beam as it is steered to large off-zenith angles. The beam directions, as displayed in Table 6.2, indicate that beam zenith angles significantly greater than 30° are used post 03:00 LT. At these angles the transmitted beam's polar diagram deviates
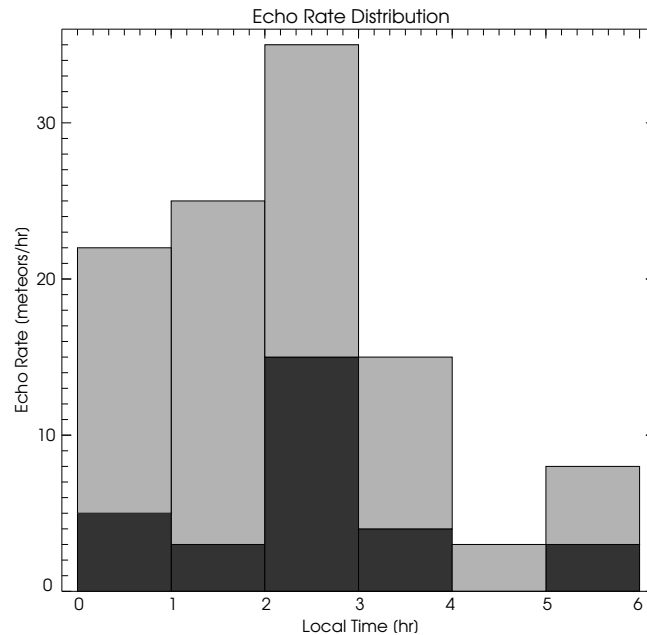
Figure 7.4: Hourly echo rate. Orionids-P (dark shaded) and total (light shaded). Note that the hourly rate from 5-6 LT is artifically reduced due to the termination of observations at 05:40 LT to exclude ionospherically contaminated echoes from the data.

significantly from its optimum form.

Recent research into the radar response function allows this current result to be placed in perspective [*Cervera et al.*, 2003; *Cervera & Elford*, 2003]. These researchers describe a theoretical formulation of response function incorporating a non-uniform meteor ionisation profile and predict echo rates for the Orionids peak of 22nd October 1997 for the radar configuration used by *Tsutsumi et al.* [1999][1]. In their analysis the predicted rates are compared with the existing observations of *Tsutsumi et al.* [1999]. Figure 7.5 displays these results as expected (dashed) diurnal variation of a sporadic source for the four combined beams, normalised to the total number of echoes, and the observed (solid) case.

To enable a comparison with this research, the approximate form of the sporadic hourly echo rate of 22 October 2000 data is obtained by subtracting the Orionids-P component (dark) from the total (shaded) component of Figure 7.4. This has the effect of shifting the initial total background peak to a sporadic peak 1-2 LT (22 echoes).

---

[1] *Tsutsumi et al.* [1999] used beams steered north, east, south and west at 25° zenith angle.

When comparing this approximated sporadic hourly rate with that of the expected (dashed) diurnal variation of Figure 7.5, the theoretical peak rate is slightly delayed in comparison to that observed. A significant difference between the expected and observed data of 22 October 1997 and the current observations is the much reduced observed minimum echo rate over 4-5 LT in the 22 October 2000 data. A slight echo minimum is predicted at 4 LT but is not observed in the 22 October 1997 data.

Figure 7.6 displays the expected hourly echo rate variation over the full 24 hr period for an east beam ($25°$ zenith angle) on 22 October 1997. The pre-sunrise behaviour is seen here again but the predicted dramatic echo rate peak from 6-8 LT indicates the extent of meteor echoes generally obscured by the ionosphere.
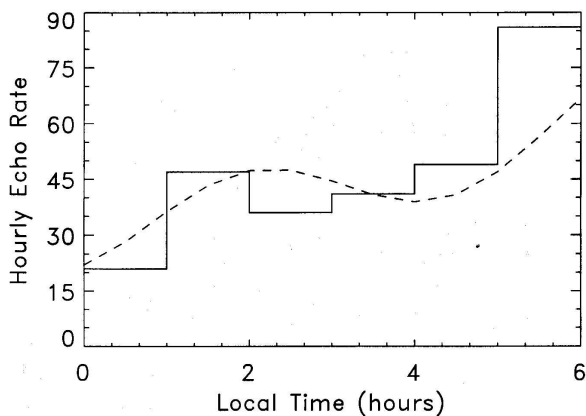

Figure 7.5: Comparison of the 22 October 1997 observed echo data (solid) [*Tsutsumi et al.*, 1999] and expected (dashed) diurnal variation of sporadic source for the four combined beams [*Cervera et al.*, 2003].
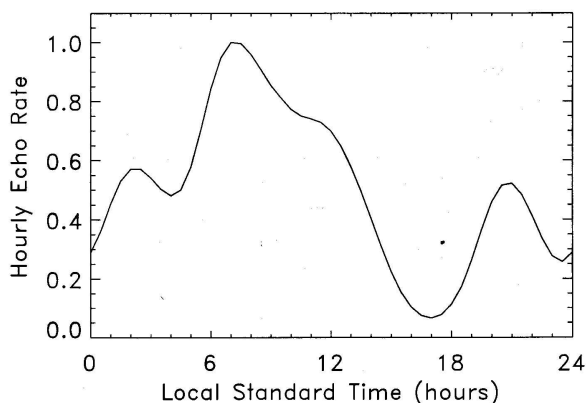

Figure 7.6: Expected diurnal variation (normalized to the peak rate) of sporadic echo rate for the east beam on 22 October 1997 [*Cervera et al.*, 2003].

It should be noted that the Orionids peak for radio observers has been predicted from the astronomical aspects to be from 2-3 UT on October 21 [*McBeath & Arlt*, 2000]. This corresponds to 11:30 to 12:30 LT 21.10.00, at which time the radiant

has set at the site and is thus not detected. In addition to this, observations are not possible at this frequency over this predicted peak in activity due to the dominant presence of the ionosphere during daytime.

7.3.3 Echo range and height distribution

The upper panel of Figure 7.7 displays a distribution of the radar range gates in which a meteor echo was initially detected. As discussed previously, the radar pulse width and range sampling interval used dictates that most meteor trails were oversampled in range, so a single range (and thus height) was determined from the range gate having the highest SNR. Also the sampling start range was varied with beam angle. This was initiated to ensure data were collected in the atmospheric region most likely to yield meteor echoes, i.e. above 80 km altitude and in consideration of the data collection limitations outlined previously (i.e. a limited data transfer rate dictated sampling range was constrained to 66 ranges, see e.g. section 2.3.6). This resulted in the range interval of data collected adjusting every 30 minutes and is indicated in Table 6.2. The selected Orionids-P component in this range distribution is well contained within the total distribution but has no definite structure as such.

The lower panel of Figure 7.7 displays the meteor height distribution obtained from the range gate and zenith angle of the reflection point location. The total distribution (light) forms a peak around $H_{Total} \simeq 105$ km and displays a roughly Gaussian appearance. Echoes were detected over the height range 65 to 132 km. The selected Orionids-P component shows a distinct grouping between 98 and 120 km, with two peaks in this distribution. Removal of the Orionids-P group leaves a sporadic distribution with a peak at 105-106 km.

Some sporadic meteoroids are observed to ablate at significant heights (i.e. $\geq$120 km). While stony meteoroids have been shown to begin to ablate at heights less than approximately 120 km (see Figure 5.5 in section 5.2.1.2), meteoroids constituted of largely organic compounds are reasoned to ablate at higher altitudes due to their lower temperature melting points (see *Elford et al.* [1997]). An example of a meteoroid shower
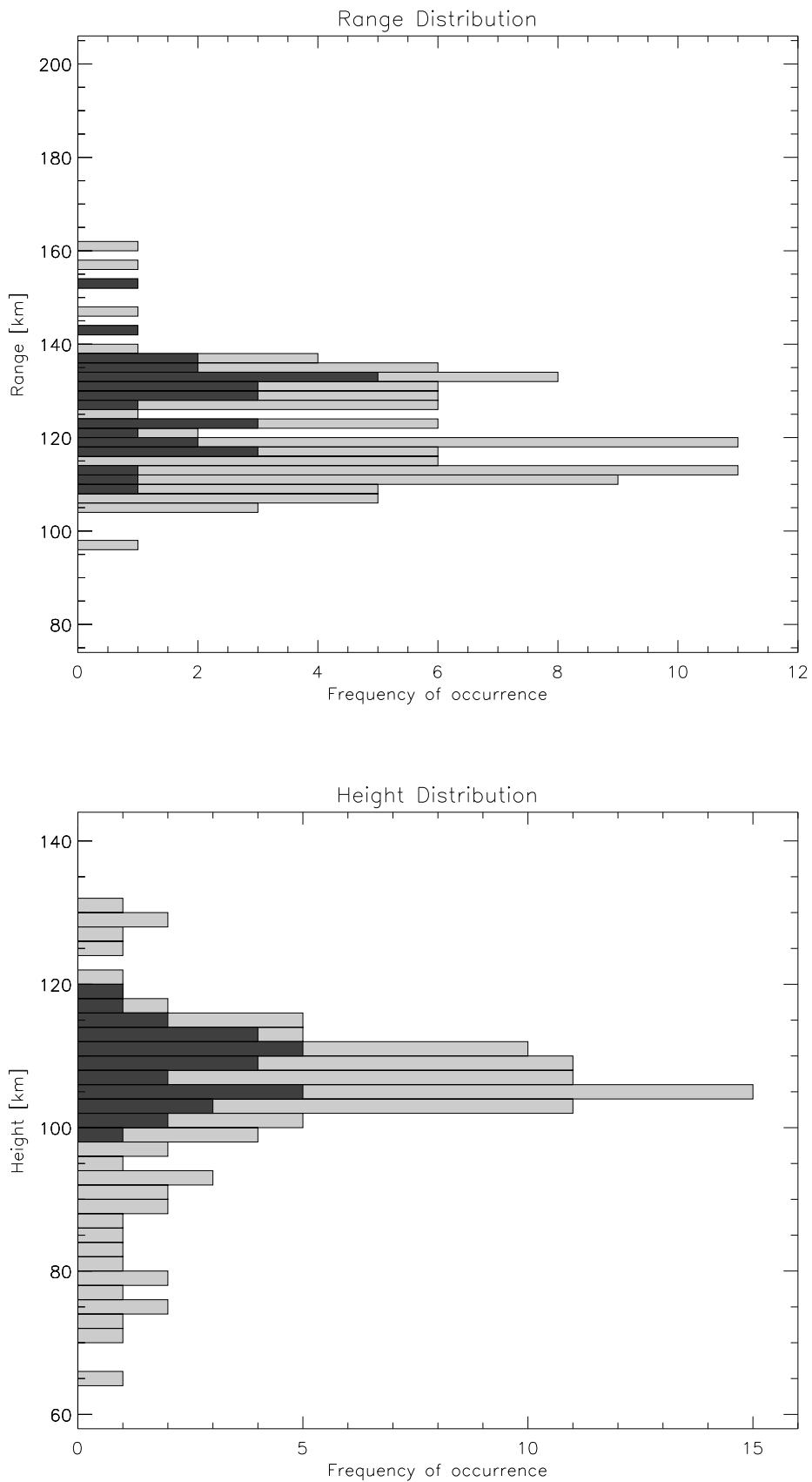
Figure 7.7: Range (upper diagram) and height (lower panel) versus frequency of occurrence. Ranges and heights are binned at 2 km intervals. Orionids-P (dark) and total (light) echoes are indicated.

with an anomalous high altitude ablation regime is that of the Draconids [*Lebedinets*, 1991] and it is supposed that these meteoroids consist mainly of organic compounds C, H, O, N (hence the term "CHON" particles).

Experimental comparison

It is scientifically valuable to compare the height distribution shown in Figure 7.7 with that of others obtained at 1.98 MHz. Using early morning observations made between April and August 1971, *Brown* [1976] produced two height distributions; one for fast rising echoes (suspected meteors) and one for slow rising echoes (possibly old meteor trails or weak sporadic *E*-layers). The former peaks around 102 km (295 meteors) and the latter about 95 km (312 echoes). Few meteors were seen above 110 km.

A later study from the same site utilised observations during the η-Aquarids shower of 1985 and other night time showers through July and August of that year [*Olsson-Steel & Elford*, 1987; *Steel & Elford*, 1991]. Echoes were detected in the height range $70 < h < 140$ km with a peak at ~ 104 km (1461 meteors) from a corrected height distribution[2]. Instrumental limitations precluded observations above 140 km.

The η-Aquarid shower was re-visited in 1986 with observations taken from 1-8 May [*Steel & Elford*, 1991]. A corrected height distribution showing no clear peak was the result, with unambiguous meteors demonstrating an almost invariant flux at all heights $100 < h < 120$ km (857 meteors in total). During the Orionids shower of 22 October 1997, *Tsutsumi et al.* [1999] detected underdense echoes over the period 00:45-05:46 LT and height range 80 to 120 km and found a mean height of 104.4 km, noting that less than 40% Orionids meteors contribute to this distribution.

Theoretical comparison

The current observations can be compared with theoretical expectations. For stony meteoroids *Ceplecha et al.* [1998, Figure 5] give the height of point of maximum ionisation as a function of speed and a similar example is also given by *Taylor & Elford*

---

[2]See *Olsson-Steel & Elford* [1987] for details of the various height corrections applied.

[1998, Figure 1]. Of the meteoroid sources discussed in section 5.2.1.1, *Taylor & Elford* [1998] nominate the helion/anti-helion and pair of apex sources as the major sources. These researchers indicate that the encounter speeds of helion/anti-helion meteoroids range between 10 and 40 km s^{-1} with a median value of 20 km s^{-1} and the apex meteoroids are 50-70 km s^{-1} with a median value of $\sim$60 km s^{-1}. The mean speed for the Orionids meteoroids is 65-67 km s^{-1}. For a maximum line density of 10^{12} electrons per metre the height of maximum ionisation for a speed of 20, 40, 60 and 65-67 km s^{-1} is 86, 97.5, 105 and 107 km respectively [*Ceplecha et al.*, 1998].

In general terms it can be seen that the Orionids-P component has a mean height of $H_{O-P} \simeq 108$ km. This component will later be shown to have a mean speed of $\sim$60 km s^{-1}, and thus there is general agreement with the theoretical height expected of such meteoroids. As mentioned, if this Orionids-P component is subtracted from the total distribution, then the sporadic background is seen to peak near $H_s = 105$-106 km. This is consistent with previous experimental observation but is significantly higher than that predicted for sporadic meteoroids with a lower mean speed of ~ 20 km s^{-1}, assuming a predominantly helion/anti-helion source.

Another theoretical analysis gives the average echo height of meteors as a function of radar frequency [*Thomas, Whitham & Elford*, 1988];

$$h = -17 \, log_{10} \, f + 124 \qquad\qquad (7.1)$$

where h is in km and f is in MHz and is based on measurements at frequencies greater than 17 MHz. For the current radar system (1.98 MHz) this results in an expected height of 118 km and over 10 km higher than that observed, which may indicate that expression 7.1 is not applicable below 17 MHz considering much of the data discussed here at 1.98 MHz.

The higher observed height of the estimated sporadic background ($H_s = 105$-106 km) can be understood in terms of the radar detectability of meteors and the selection bias imposed by the ablation characteristics of meteoroids. *Taylor & Elford* [1998] have investigated the selection effects associated with radar observations in a

re-analysis of the Harvard Radio Meteor Project data. A primary consideration for radar meteor data is that a meteor's detectability is $\propto q_{max} \propto V^{3.75}$, where q_{max} is the maximum electron line density of the trail and V is the speed of the meteoroid. Thus for a particular mass range, a meteoroid's detectability is many times greater for a meteoroid travelling at 60 km s^{-1} than one travelling at 20 km s^{-1}. So it is expected that there exists a higher proportion of faster sporadic meteoroids than slower ones in the radar observations presented here and that these faster meteoroids ablate at higher altitudes.

It should be noted here that the non-ideal radar environment of the upper atmosphere is characterised by absorption by D-region layers and path altering effects of E-region structures (including signal retardation[3]) for instance. Such effects have been thoroughly discussed in *Steel & Elford* [1991]. These researchers state that atmospheric ionisation can cause significant retardation, refraction and/or absorption of the transmitted radio waves. Retardation and refraction could lead to the apparent height of the meteor train being higher than its true altitude, while absoprtion can lead to attenuation of the returned echo signal and thus reduce the detection of some meteors. Refraction may also lead to the actual reflection point being displaced from the linear geometry case.

Evidence on the impact of the ionosphere on calculated night-time meteor heights has been determined to be negligible when ray paths are calculated using a night-time electron density profile and transmitted ray angles of 20° from the zenith [*Meek & Manson*, 1990]. However the variability of atmospheric ionisation with time and geographic location may modify this assertion.

To improve the quality of height data in future studies a number of approaches may be trialled. Observations may be taken on ionospherically "quiet" nights or additional quality control checks made on echo data. Quality control checks may take the form of internal validation or independent comparison of derived height such as: 1) decay

---

[3]*Stubbs* [1973] notes that at night 2 MHz radio waves are totally reflected from the F-region near a height of 230 km.

times; 2) calculated shower height range; 3) winds; 4) ionospheric layer prediction; 5) ray modelling; 6) data self-consistency; 7) magnetic field effects and 8) range bracketing at a higher frequency. These are outlined in Appendix K.

Because of the alternate uses of echo decay times (e.g. diffusion coefficients etc.) this method of echo height validation was explored further in this study. Echoes from 22 October 2000 were examined for typical underdense behaviour, i.e. echo amplitude peaks, followed by an exponential decay from which a time constant can be determined. Few meteors displayed this model characteristic to allow for a decay time to be determined. Primary differences between model behaviour and the data examined were the lack of a clear exponential decay, suspected to be due to the long duration of echoes at MF frequencies giving time for trail distortion to occur. The lack of suitable echoes has been observed before in 1.98 MHz meteor data where it also precluded decay times from being determined [*Olsson-Steel & Elford*, 1987]. A study by *Brown* [1976] noted that only a small group of echoes (35 from a total of 295) satisfied the model characteristics for an underdense echo such that time constants could be deduced. In addition to the likelihood of few decay times being available, there are further considerations necessary when applying these times for height validation which are outlined in *Ceplecha et al.* [1998].

7.3.4   Echo occurrence time vs height

Figure 7.8 displays the meteor echo start time plotted against height. The form of the data collected has some bearing on trends evident in all subsequent plots where time is the abscissa and this should be highlighted here. As discussed in section 6.1.3 the meteor time series collected were 58.3 seconds followed by a dead-time of 101.7 seconds. However the dead-time is not represented on this and similar plots in order to provide better overall clarity. So any apparent vertical alignment of meteor events in the data are thus attributed to the isolated meteor time-series representing only a fraction of the contiguous time axis. Note, as shown in the next section, no durations exceed 14 seconds for Orionids-P meteors.
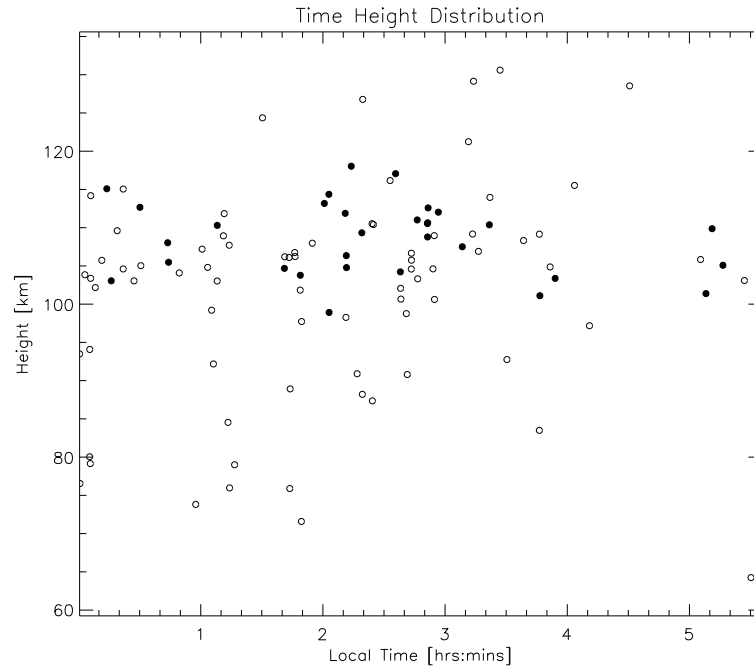
Figure 7.8: Orionids-P echo time vs height. Orionids-P (filled) and total population (unfilled) are indicated.

7.3.5 Echo duration distribution

Echo durations were also examined and are displayed in Figure 7.9. In this study, duration was defined to be the bulk time difference between the first emergence of the meteor amplitude from the surrounding noise to the point where the signal again falls below this level. There exists numerous meteor time measures, however the above definition most closely resembles that of the echo duration of an overdense trail (T_{ov}) as given by *McKinley* [1961]. In contrast to this is the echo decay time (T_{un}) of an underdense trail which is measured from the time of maximum amplitude to the time when the amplitude decays to a given arbitrary fraction of the peak, most often $1/e$ where e is the base of natural logarithms [*McKinley*, 1961]. This echo decay time was not able to be consistently measured in this study, hence the substitution of the more robust bulk duration measurement. Echo decay times are typically of the order of seconds at MF, while echo durations can range from seconds to minutes. As defined, duration is in fact a measure of both meteoric and atmospheric characteristics (i.e. it measures meteoric ionisation endurance) in that the initial increase in echo power due

to the meteoroid is often maintained as the trail persists and drifts with the neutral wind. It should be noted that in this study a small number of measured durations are artificially short due to the echo amplitude series being terminated at the end of the acquisition.

Two-to-three seconds is perhaps an indication of the most expected duration of a meteor event, while the spread of longer times (up to 13.5 seconds) tends to indicate the relative endurance of individual drifting trails. The fact that the majority of trails detected at medium frequency have a duration of less than fifteen seconds is an observation also made by *Brown* in *Briggs et al.* [1972]. *Baggaley* [1978] also noted that HF meteor echoes rarely exceed a duration of 1 minute and discussed the influence of meteoric and atmospheric chemistry on this duration. The longer duration trails are also subject to severe fading as atmospheric winds distort the trains creating multiple reflection centres [*Poulter & Baggaley*, 1977].

The selected Orionids-P component displays a similar form to the total, with most echoes exhibiting short durations. Here, 50% of the Orionids-P echoes have a duration
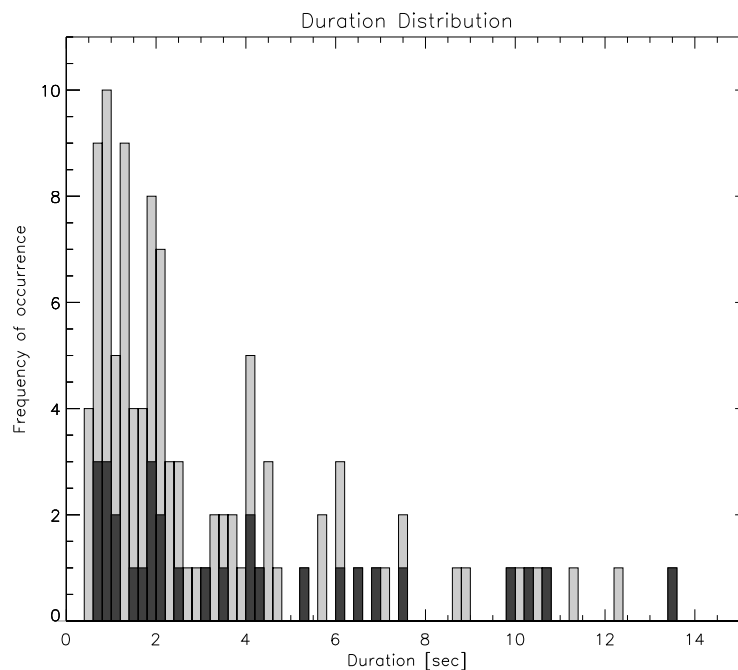

Figure 7.9: Echo duration vs frequency of occurrence for Orionids-P (dark) and total sample (light).

less than ∼2 seconds and two-thirds have durations less than 5 seconds.

Figure 7.10 displays the bulk duration versus height. If duration measurements are expected to display some trends similar to decay times, then short duration meteors are expected to occur at high altitudes and longer duration meteors will occur at lower altitudes. This general form is displayed in Figure 7.10, although it is clear that bulk duration is not as sensitive a measure as decay time. Most Orionids-P meteors are of a short duration confined to the 100 to 120 km region.

7.3.6   Speed distribution

The distribution of meteoroid speeds for the data set, calculated via the Fresnel phase time technique (see section 6.3.3), is displayed in Figure 7.11. Distribution bin size is 5 km s^{-1}. The majority of meteoroid speeds are contained within the expected heliocentric parabolic speed range of 11 to 74 km s^{-1}. The total sample speed distribution (light shaded) has a spread around ∼50 km s^{-1}. If the Orionids-P component (dark shaded) is subtracted from this total distribution, it is apparent the mean peak value
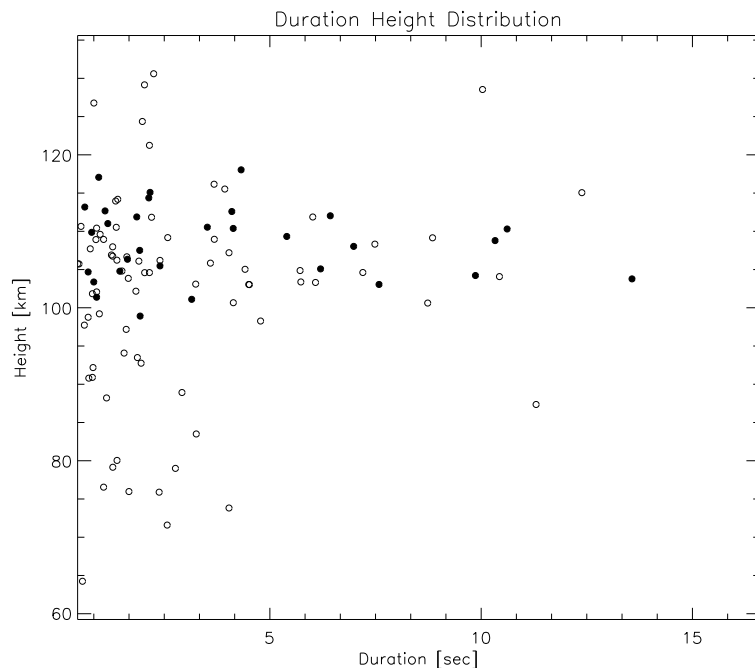

Figure 7.10: Echo duration vs height for Orionids-P (filled) and total sample (unfilled).

of a roughly Gaussian sporadic distribution is shifted towards a lower speed of 40-45 km s^{-1}. As discussed in section 7.3.3, radar observations of meteoroids are biased toward the detection of fast meteoroids. This accounts for the sporadic mean speed observed here being significantly higher than the $V_s = 20$ km s^{-1} expected from a predominantly helion/anti-helion source [*Taylor & Elford*, 1998]. Two distinct speed groups can be identified in the Orionids-P component; a dominant speed group from 45-80 km s^{-1} centred around ~60 km s^{-1} and a smaller low speed component from 25-40 km s^{-1}.

The dominant group of selected Orionids-P meteoroid speeds is also in general agreement with the expected mean Orionids meteoroid speed of 65-67 km s^{-1} and confirms the detection of the Orionids stream during this observation period.

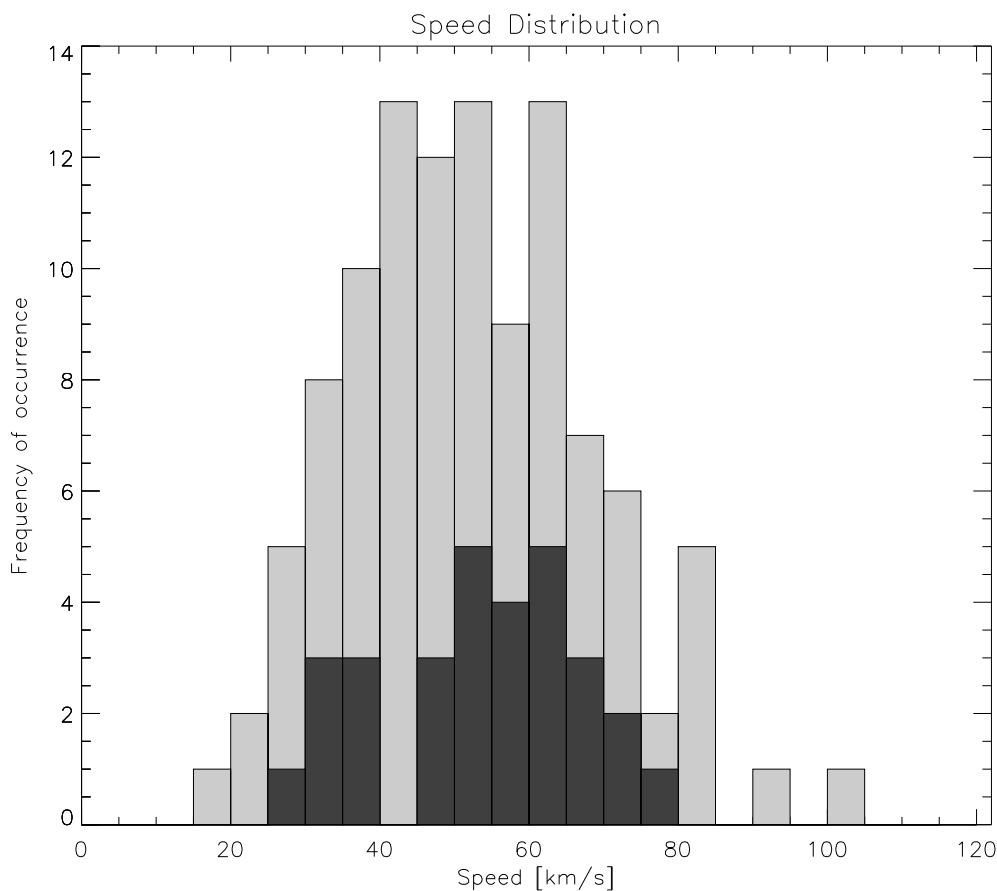The radiant technique of *Elford* [1954] has selected mostly meteors with speeds

Figure 7.11: Meteoroid speed vs frequency of occurrence. Orionids-P component (dark shaded) and total (light shaded). Bin size is 5 km s^{-1}.

related to the Orionids shower, however the presence of the low speed group within the selected Orionids-P meteor component is an interesting feature. This sub-structure may arise 1) from an established or previously unrecognised meteoroid stream or 2) due to sporadic meteoroids having echo coordinates that align with the Orionids by chance. Radio meteor studies (e.g. *Nilsson* [1964]; *Gartrell & Elford* [1975]; *Sekanina* [1976]) were examined for any evidence of low speed showers active during the October period commensurate with the Orionids shower. No likely corresponding showers were found.

To address the question of whether these few low speed meteors have echo coordinates similar to that of the Orionids by chance, the meteors were divided into appropriate speed groups and re-plotted on the celestial polar diagram with the Orionids-P radiant. Four speed groups were used (11-25, 25-45, 45-80, $\geq$80 km s^{-1}) and are displayed in Figures 7.12 to 7.15. If the low speed meteors ($<$45 km s^{-1}) are contained within the "radiant group" by chance, then it is expected that all such low speed meteors would be randomly distributed throughout the plot area, with no significant increase in position "density" within the confines of the selected Orionids-P radiant. The previously noted partial clustering of all meteor echoes due to radar site geography must also be included in this consideration. In addition to this, as the meteor echoes have been classified according to their speed and displayed in celestial polar coordinates, meteor showers will again be indicated by the selected meteors forming a line.

Examining each figure in turn, Figure 7.12 ($11 \leq V < 25$ km s^{-1}, $N = 3$) shows that no very low speed meteor echoes are contained within the defined Orionids-P radiant and that there is no defined structure to those few meteors that are contained within this speed group.

Figure 7.13 ($25 \leq V < 45$ km s^{-1}, $N = 36$) (filled) displays a significant portion of the total echoes (33%). The indicated echoes cover most areas of the observation but do not have any significant structure. This assertion can be confirmed by estimating the expected number of non-Orionids-P (sporadic) meteors that are likely to be contained

within the selected Orionids-P radiant by chance.

To determine this estimate, the "area density" of the echoes on this celestial plot is examined. A band with width equivalent to that of the radiant selected is positioned incrementally at multiple declinations either side of the selected radiant so as to cover all meteor echoes in this diagram. At each declination increment, the total number of echoes contained within the band are counted. Thus a graph of declination increment vs echo count results. This will display a large peak at zero increment declination, indicating the presence of the Orionids shower, accompanied by a significantly lower level distribution "tail" each side of the peak. These distribution "tails" are representative of the number of background echoes over the period of observation. If an interpolation is performed across the base of the shower peak count to effectively join the two distribution tails, an estimate of the expected number of background meteors can be obtained at zero increment declination. This analysis was performed and a rough estimate of six out of the thirty Orionids-P shower meteors are reasoned to be contained within the selected Orionids-P radiant by chance, leaving 24 "true" Orionids-P members. Figure 7.13 displays a similar number of low speed meteors contained within the selected Orionids-P radiant and because of this such meteors are deemed to be not associated with the Orionid shower and are contained within the chosen radiant by chance.

Figure 7.14 ($45 \leq V < 80$ km s^{-1}, $N = 62$) (filled) meteoroid speed range was chosen as it best encompasses the Orionids-P component speeds. This speed group contains 57% of the total echoes. In this figure it appears there are two main features; a significant clustering of echoes along the radiant line indicated, and echoes outside this radiant appear randomly distributed. If the coordinate transform technique has indeed selected the Orionids component well, it is expected that the radiant constrains a significant number of Orionids speed meteors within the radiant. This is clearly shown here.

Figure 7.15 ($V \geq 80$ km s^{-1}, $N = 7$) (filled) shows that all high speed meteors are randomly distributed in terms of their celestial observation coordinates. Note that five

of the seven echoes appear within the selected radial axis range of $|\tan\alpha| = 2.2$, while two lie outside this range. The two echoes however do not contribute to identifying any structure in this speed group.

Figures 7.16 ($45 \leq V < 60$ km s^{-1}) and 7.17 ($60 \leq V < 80$ km s^{-1})) are displayed to further interpret the echo distribution of speed range ($45 \leq V < 80$ km s^{-1}) of Figure 7.14. There are approximately twelve meteors (filled) contained within the Orionids-P radiant in each diagram. This number of echoes is significantly more than the estimated background derived by the previous analysis and also is a high proportion of the total number within each speed group.

While distinct trends have been identified, it is possible that an increase in the number of meteor echoes would allow any hidden structure to be firmly established and this a prime motivation for increasing the count rate at this relatively low meteor radar frequency.
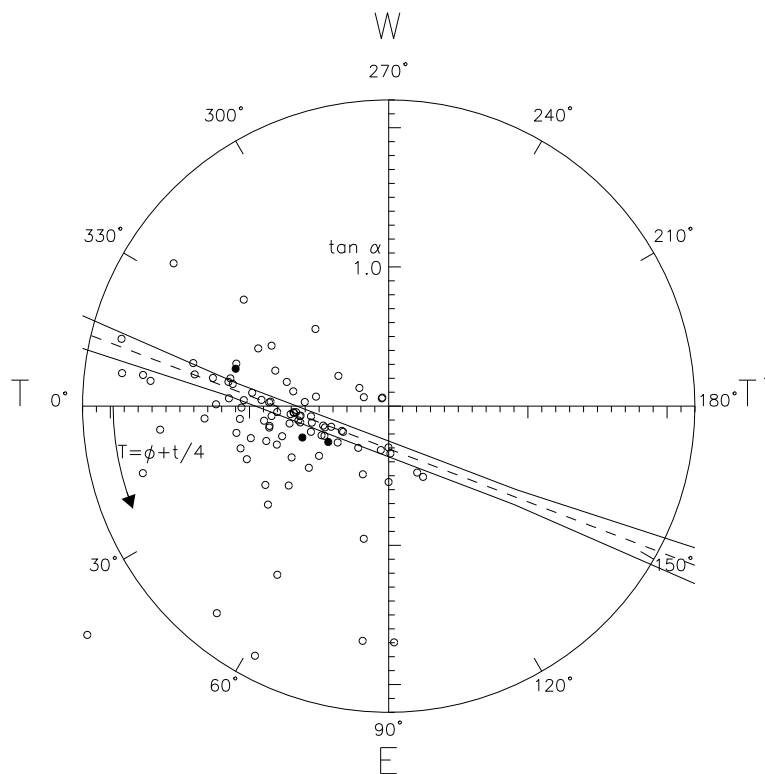
Figure 7.12: Celestial polar plot of echoes in speed group 11-25 km s^{-1} ($N = 3$) (filled) and total sample (unfilled). Orionids-P (α,δ)=(95°,16°) radiant is also indicated.
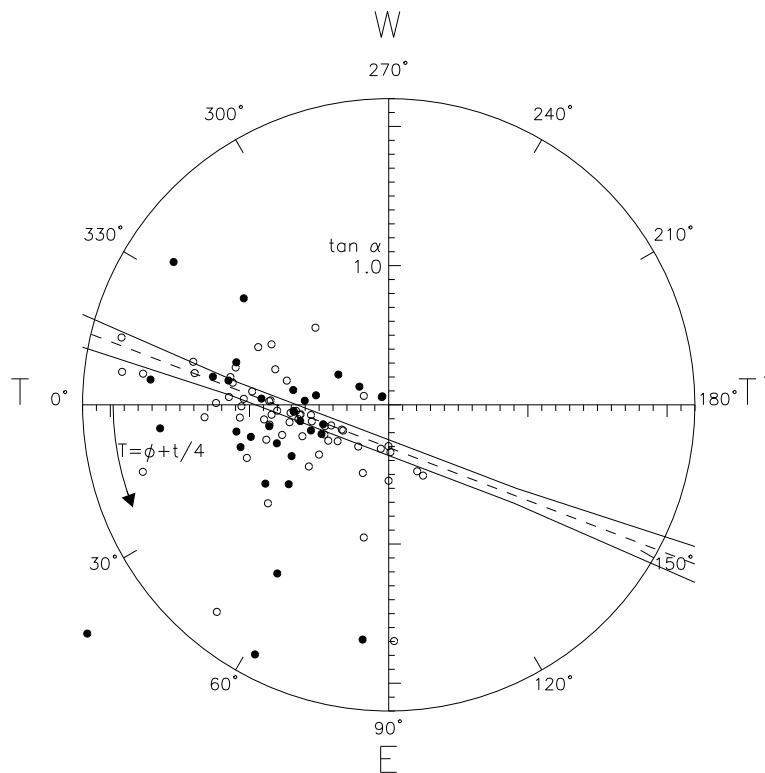
Figure 7.13: Celestial polar plot of echoes in speed group 25-45 km s^{-1} ($N = 36$) (filled) and total sample (unfilled).
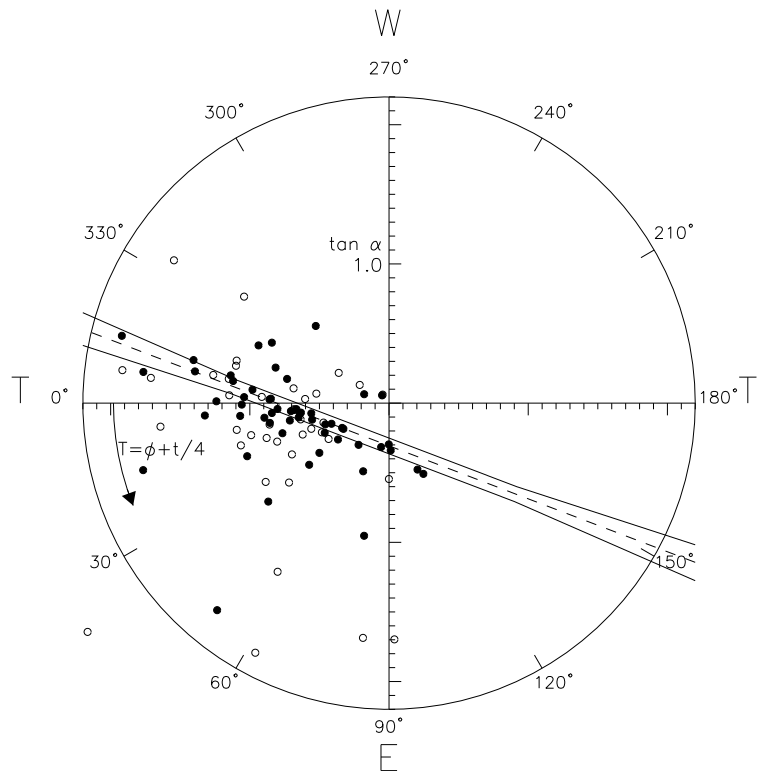
Figure 7.14: Celestial polar plot of echoes in speed group 45-80 km s^{-1} ($N = 62$) (filled) and total sample (unfilled).
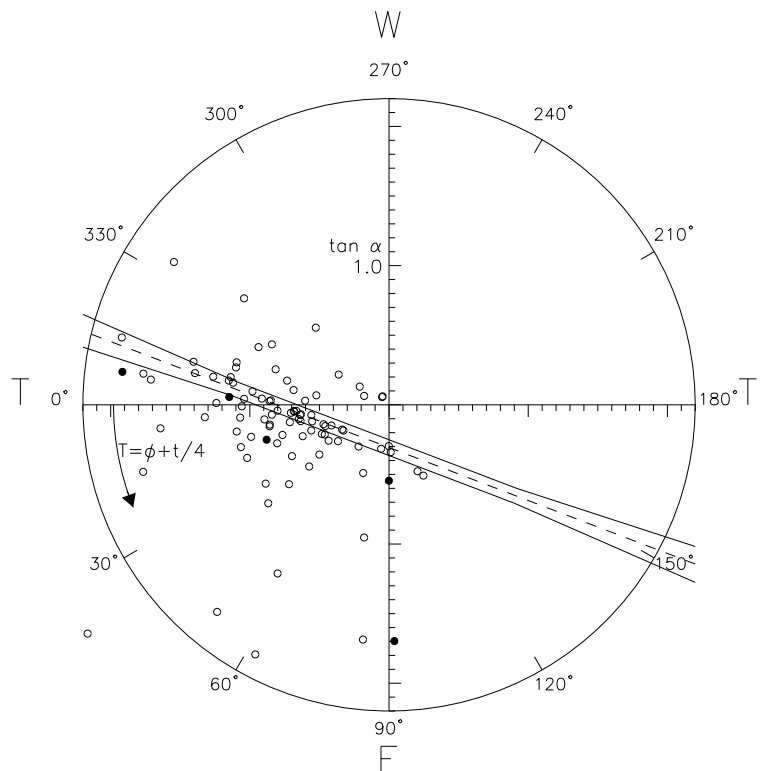

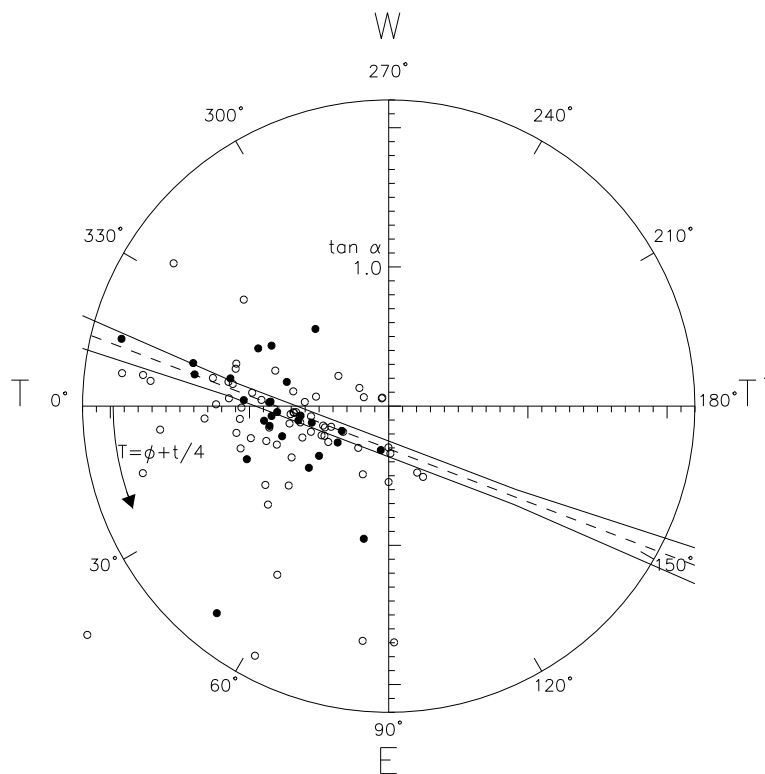Figure 7.15: Celestial polar plot of echoes in speed group $\geq$80 km s^{-1} ($N = 7$) (filled) and total sample (unfilled).

Figure 7.16: Celestial polar plot of echoes in speed group 45-60 km s^{-1} ($N = 34$) (filled) and total sample (unfilled).

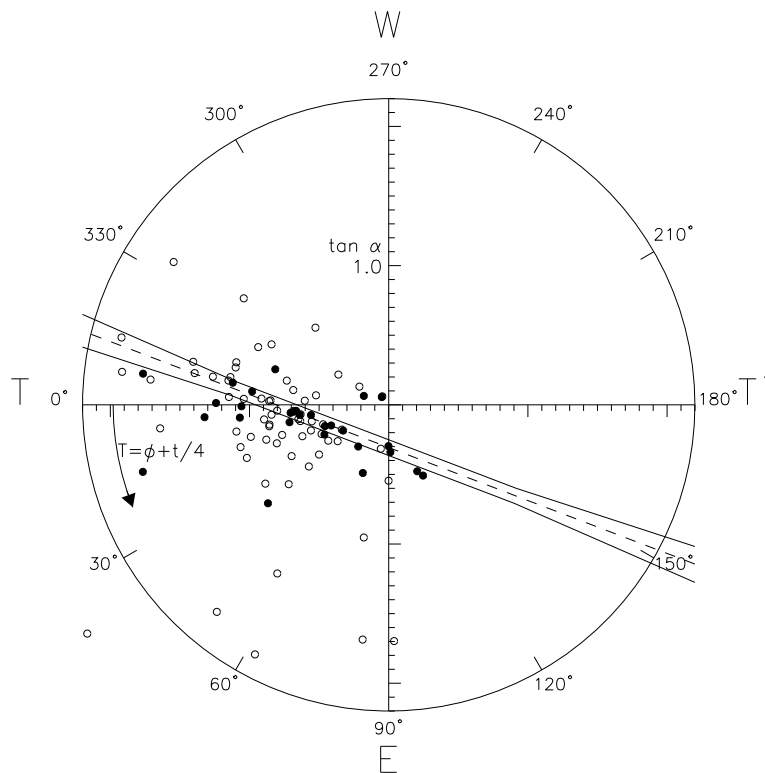

Figure 7.17: Celestial polar plot of echoes in speed group 60-80 km s^{-1} ($N = 28$) (filled) and total sample (unfilled).

Of benefit in this analysis has been the distinctly higher speeds of the Orionid stream when compared to the sporadic speed distribution and it has been noted by *Steel* [1993] that this fact has also contributed to the unequivocal linking of the Orionids and η-Aquarids to the Comet P/Halley. This exploitation of higher speed meteoroids to isolate shower activity has been achieved by others at VHF radar frequencies, such as *Singer et al.* [2001] who detected the 1999 and 2000 Leonid storms. However the separation of lower speed showers from the sporadic background may offer additional challenges.

The presence of non-heliocentric speed meteors in the speed distribution (light shaded) of Figure 7.11 is also of interest. Echoes with speeds near 80 km s^{-1} may be within the measurement errors while the velocities extending from 90 km s^{-1} decrease in frequency as speed increases to form a high speed tail of the distribution.

Discussion on the reality of an interstellar meteoroid component has continued for the last 60 years [*Baggaley*, 2000]. Meteor surveys using various observational techniques have often identified a meteoroid component with hyperbolic orbits, with this component ranging from 0% (suppressed as supposed measurement errors) to 25% of total orbits identified [*Taylor et al.*, 1994]. Recent work has indicated a source geometry of the influx of extra-solar system particles, that being from southern ecliptic latitudes containing possible discrete sources and a dominant compact directional inflow from the direction of the star β Pictoris [*Baggaley*, 2000]. Orbital data and accurate speed estimation techniques are vital in the study of interstellar meteoroids. This balance has been achieved with the AMOR radar system [*Baggaley et al.*, 1994] using the time-of-flight speed measurement technique (described in section 5.3.1.3) and more recently, using the Fresnel phase time method [*Elford*, 2003*b*, private communication].

7.3.7 Echo height vs speed

Figure 7.18 displays the speed vs height of the sample. A weak trend is evident in that faster meteoroids generally ablate at higher altitudes. The cluster of low speed meteors at 125-130 km is interesting as they cannot be stony particles. This is possible
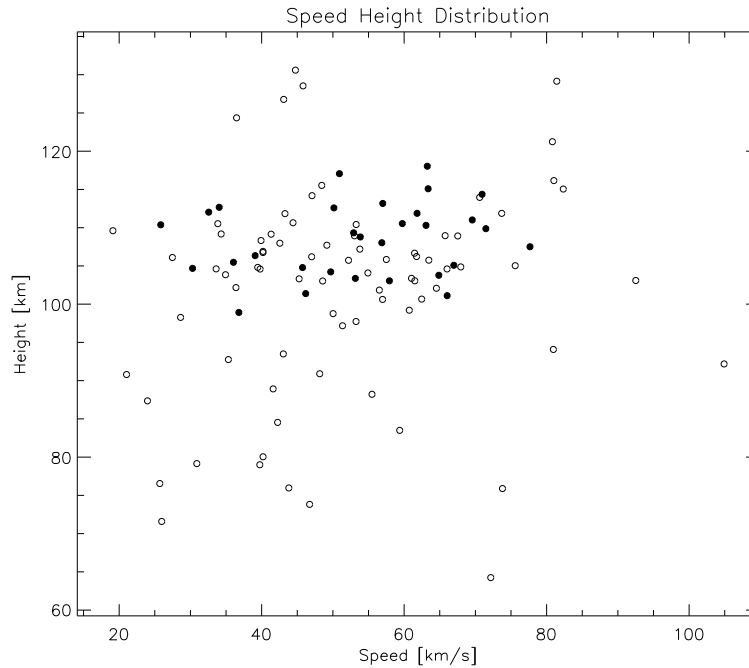
Figure 7.18: Height versus speed with Orionids-P (filled) and total sample (unfilled).

evidence of low temperature ablation meteoroids, indicative of "CHON" material. The two meteors with height less than 80 km and speed of $\sim$70 km s^{-1} cannot be explained by any accepted ablation theory.

7.4   Orionids secondary component

While the dominant structure identified in Figure 7.1 corresponds to the expected radiant coordinates of the Orionid shower, it is apparent that a second structure exists almost parallel to this. This secondary structure is best selected by a radiant of (α, δ) = (93.5, 21.0), $\Delta H, \Delta \delta = \pm 2.0°$ and the selection result is displayed in Figure 7.19. This secondary structure is designated Orionids-Secondary (Orionids-S).

Figure 7.20 illustrates the angle-of-arrival of the Orionids-S component. As in the Orionids-P component displayed earlier there appears to be a general clustering of reflection point directions.

Figure 7.21 displays the height distribution of meteors with the Orionids-S selected (dark shaded). Again, the core of this component is relatively well grouped in height

although not as clearly defined as that exhibited in Figure 7.7. Figure 7.22 displays meteoroid speeds with the selected Orionids-S component (dark) against the total sample (light). It is apparent there is a dominant group (50-75 km s^{-1}) centred around the expected Orionids speed of 65-67 km s^{-1}. Also, as in the case of the Orionids-P, there is a low speed group (20-45 km s^{-1}). It is suggested that the low speed group selected by the transform technique corresponds to echoes with coordinates similar to that of the Orionids-S by chance following a similar analysis to that described for the Orionids-P case.

Conclusion

Excluding the four sporadic low speed meteoroids identified in the speed distribution, a secondary Orionid radiant has been identified with a strength of 11/24 (∼50%) of the primary component. Thus we find that a total of 35 Orionid meteors are observed on 22 October 2000, of which ∼1/3 are in a minor filament about 5° higher in declination than the accepted radiant position (α,δ) of (95°,16°). The speed distributions are essentially the same. With this information the shower strength index (S) can be re-calculated as 35/73=48%.
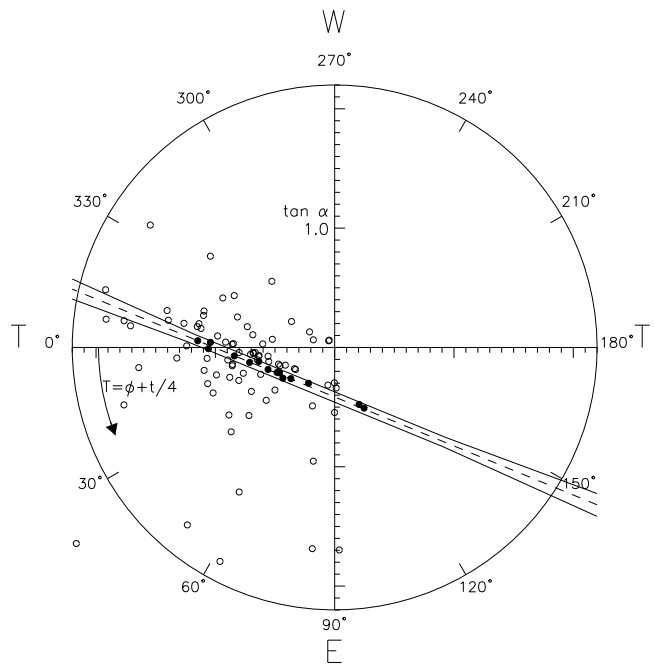
Figure 7.19: Celestial polar plot of 22 October 2000 meteor echoes including the Orionids-S radiant (93.5°, 21.0°) (dashed line) and radiant errors (solid) $\Delta H, \Delta \delta = \pm 2.0°$. Fifteen potential shower meteors are selected by this method.

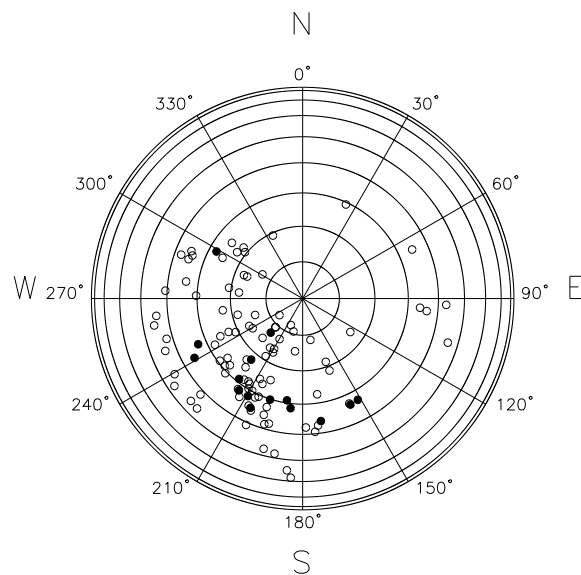Figure 7.20: Meteor reflection point angle-of-arrival 22 October 2000. Orionids-S (filled) echoes in comparison to total meteors detected (unfilled).
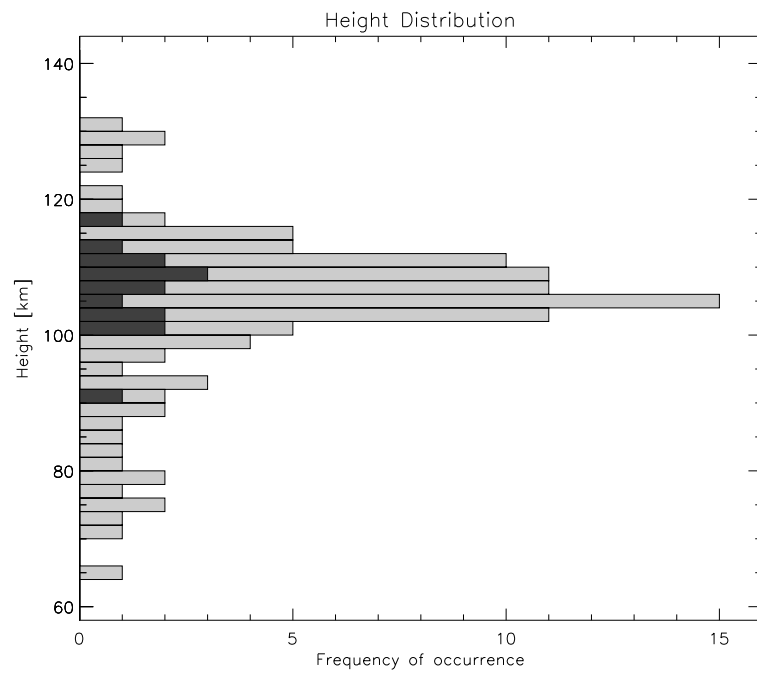
Height Distribution

Figure 7.21: Orionids-S (dark shaded) height vs frequency of occurrence. Total sample (light shaded) is also shown.
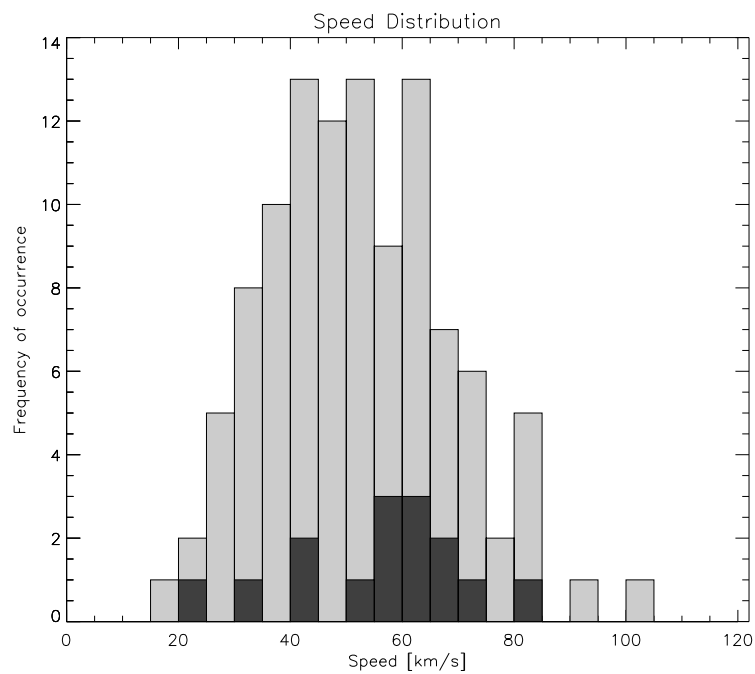
Speed Distribution

Figure 7.22: Meteoroid speed vs frequency of occurrence with the Orionids-S (dark shaded) and the total sample (light shaded).

7.5   Identification of other radiants

While the dominant structures in the celestial polar plot of the reflection point data (see Figure 7.1) have been identified, attention is now focused on the surrounding echo complex. *Jones & Morton* [1977] note that there is an increasing body of evidence to suggest that sporadic meteors are the end products of dispersed and depleted meteoroid streams. If this is the case then perhaps an indication of these or other streams is contained in the background complex presented in this study. Such an approach is also warranted in the sense that a radar meteor system is optimised to observe a different (fainter) meteoroid complex than are visual (brighter) observations for instance. This places the current radar study in a position to possibly identify shower structures that may not have been observed previously or to corroborate existing observations detected via alternate techniques.

Figure 7.23 selects a radiant defined by $(\alpha, \delta) = (67.5°, 24.0°)$. The selection of this radiant is aided by the good alignment of the majority of the echoes and the echoes at the extremities of the line. Figure 7.24 displays the speed distribution of the selected component (dark shaded) against the total (light shaded). No definite speed groupings are evident from this figure. It should be noted that some of the higher speed members in this distribution are probably "true" Orionids as the selected radiant band crosses the Orionid radiant alignment.

Figure 7.25 displays the selected radiant of $(\alpha, \delta) = (103.0°, 25.0°)$. Here an increase in radiant error was utilised to encompass those echoes apparently distributed around a common line. Again, outlying echoes assisted in the radiant selection. Figure 7.26 displays the speed distributions associated with this possible radiant. No particular speed groupings are evident from the figure although as mentioned above, some higher speed members are likely to be Orionids shower members.

In a similar orientation to that described in the previous case, Figure 7.27 shows a collection of echoes apparently evenly distributed around a particular radiant, given as $(\alpha, \delta) = (80.5°, 55.5°)$. Figure 7.28 displays the speed distribution of the meteoroids,

which does not show any particular grouping.

It is apparent from the above analysis of the background radiant structure here that an increase in meteor echo counts, coupled with observations over consecutive days would serve to more readily confirm or deny these or other possible structures.

Figure 7.23: Celestial polar plot of 22 October 2000 meteor echoes identifying the possible radiant $(\alpha,\delta) = (67.5°, 24.0°)$ (dashed line) and radiant errors (solid) $\Delta H, \Delta \delta = \pm 2.0°$. 13 meteor associations (filled) are selected.

Figure 7.24: Meteoroid speed vs frequency of occurrence for possible radiant $(\alpha,\delta) = (67.5°, 24.0°)$ component (dark shaded) and total (light shaded). Bin size is 5 km s^{-1}.
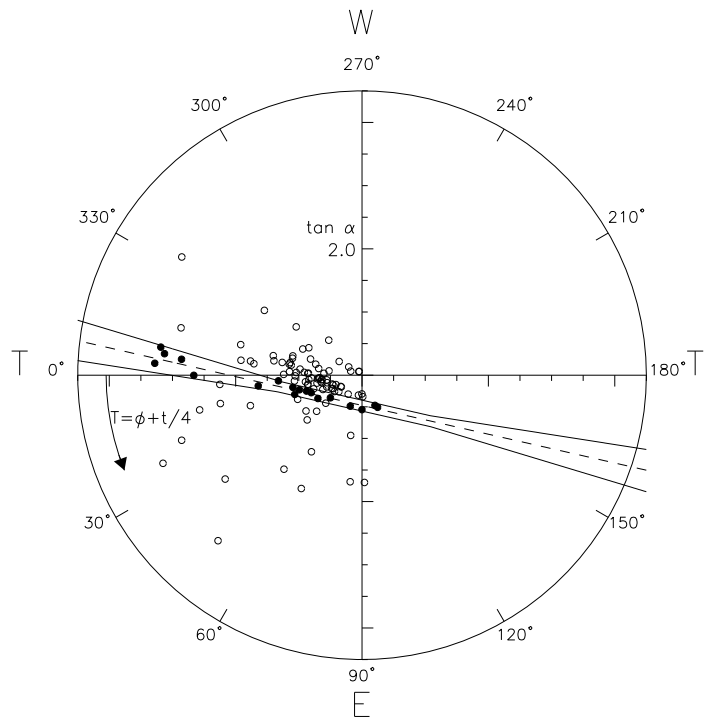
Figure 7.25: Celestial polar plot of 22 October 2000 meteor echoes identifying the possible radiant $(\alpha,\delta) = (103.0°, 25.0°)$ (dashed line) and radiant errors (solid) $\Delta H, \Delta\delta = \pm 3.95°$. 18 meteor associations are selected.
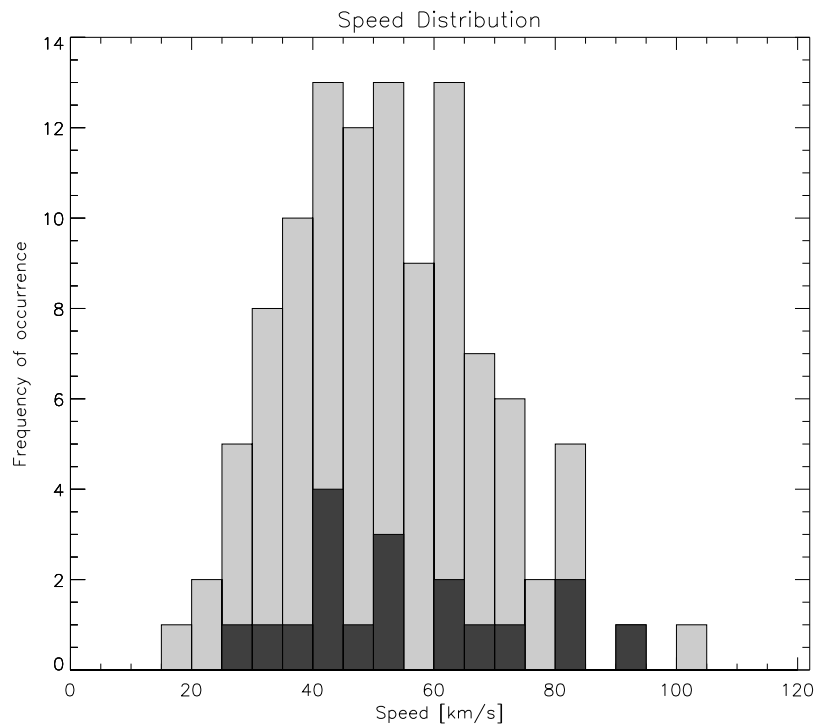
Figure 7.26: Meteoroid speed vs frequency of occurrence for possible radiant $(\alpha,\delta) = (103.0°, 25.0°)$ component (dark shaded) and total (light shaded). Bin size is 5 km s^{-1}.
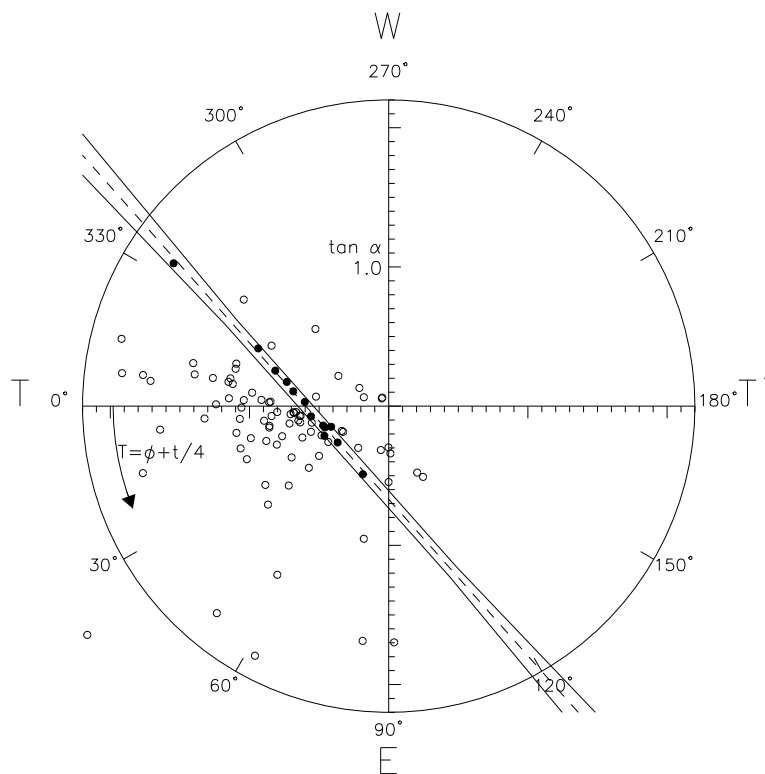
Figure 7.27: Celestial polar plot of 22 October 2000 meteor echoes identifying the possible radiant $(\alpha,\delta) = (80.5°, 55.5°)$ (dashed line) and radiant errors (solid) $\Delta H, \Delta \delta = \pm 2.5°$. 9 meteor associations (filled) are selected.

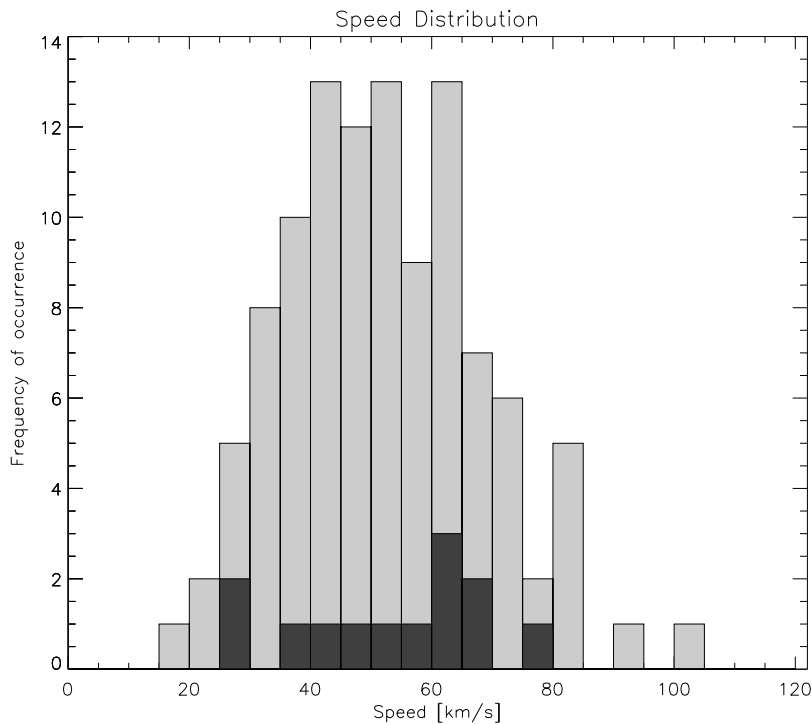
Figure 7.28: Meteoroid speed vs frequency of occurrence for possible radiant $(\alpha,\delta) = (80.5°, 55.0°)$ component (dark shaded) and total (light shaded). Bin size is 5 km s^{-1}.
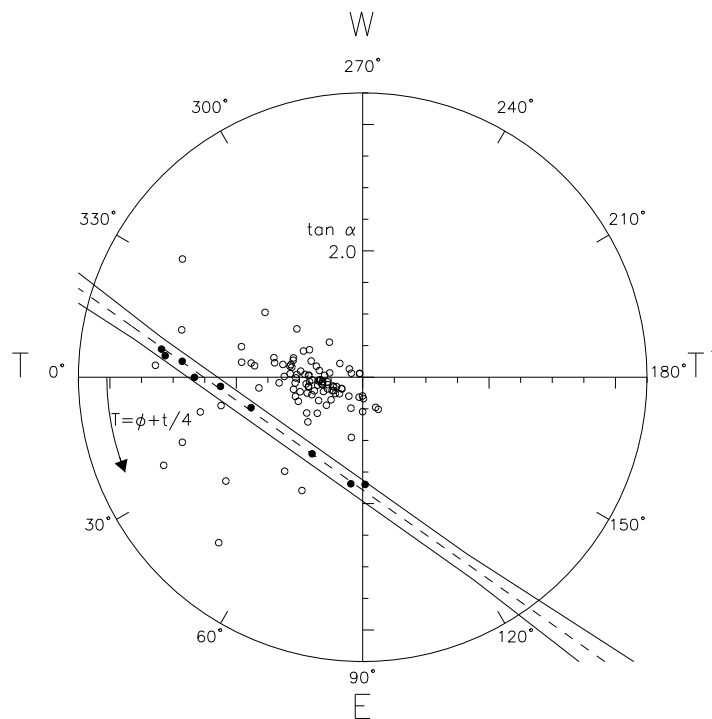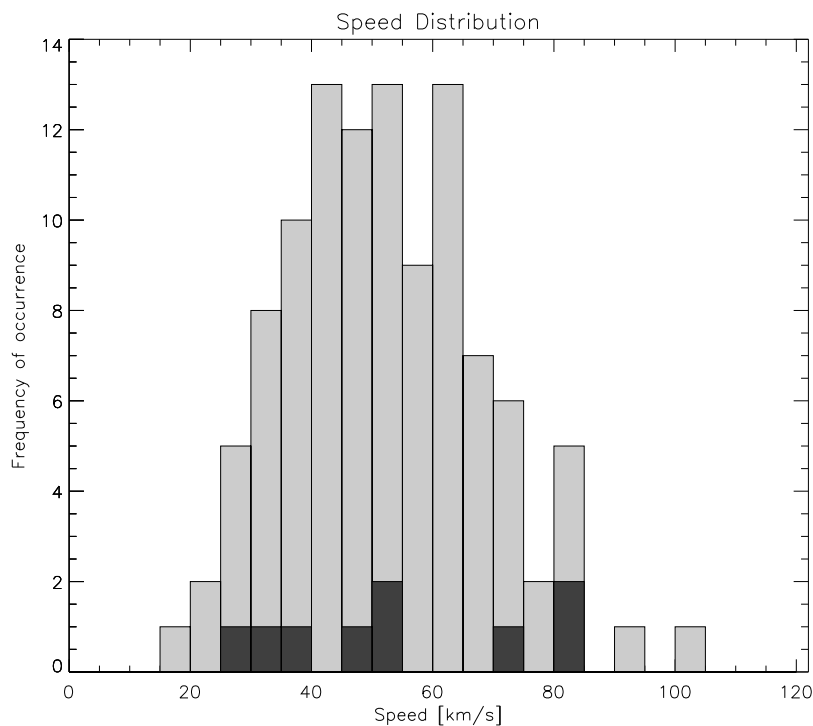
7.6 Summary

From the data presented in the previous sections the transform technique of *Elford* [1954] has been successful in selecting those echoes belonging to the Orionids meteoroid stream from the general complex observed on 22 October 2000. There has been good agreement between the experimentally derived distributions of meteor echo angle-of-arrival, height and speed for this Orionids-P component and theoretical expectations. A primary characteristic of Orionids-P component is its well grouped nature on many of these distributions of meteor parameters. In particular, the Orionids-P component speeds selected by this technique, were found to be distributed around a mean speed similar to that determined by other meteor observational methods of the Orionids. Also apparent in this speed distribution is a small low speed component. Meteor speeds were then plotted according to some defined speed groups in order to isolate the origin of this low speed group. This form of data presentation suggests that the low speed group was due to sporadic meteors included in the radiant group by chance.

The characteristics of the sporadic background observed during this early morning period appear to exhibit the known radar observational bias towards faster geocentric meteoroids. Here, the sporadic speeds centered on approximately 40 km s^{-1}, is significantly higher than the expected mean sporadic speed of the helion/anti-helion component of 20 km s^{-1}, with a consequent increase in heights of meteoroid ablation.

A second significant structure was discerned from the celestial polar plot of the data, termed Orionids-S. The orientation of this secondary feature, being almost parallel in alignment (i.e. similar right ascension, distinct declination), together with a significant number of its constituent echoes having meteors speeds in agreement with the expected Orionids stream, suggests a common stream parentage. This is an interesting result in light of the findings of *Lindblad & Porubcan* [1999] who have re-visited the extensive visual data focused on the Orionids and can find no substantial evidence of a very complicated radiant structure.

An explanation for the two separated structures identified here is that there is a

difference between the visual (photographic and video) meteors detected and radar studies, in that they detect slightly different components of the Orionid meteoroid stream. In this respect *Porubcan* [1973] has reported that the radiants of faint (Orionids) meteors are more dispersed than those obtained from brighter photographic observations.

The validity of other associations, indicating possible meteoroid streams observed in this study, are less well supported by the evidence. Their identification here has been based primarily on "associations" on the celestial polar diagram, and here the low meteor count rate at MF is a particular disadvantage. Also, distributions of meteor angle-of-arrival, height etc., have not been instructive in isolating other characteristics of these possible streams. As indicated previously, if such streams have characteristic speeds near the sporadic distribution mean speed, then their isolation using this technique and single station radar data is not straightforward. In such cases meteoroid orbit data is vital.

The coordinate transform technique of *Elford* [1954] (and later of *Jones & Morton* [1977]) is appropriate for application to reflection point data gathered by a medium frequency radar. Identification of weak showers is possible and the technique is flexible in the sense that meteor echoes can be readily included or excluded from the desired radiant by the relaxing or tightening of the radiant errors. While the technique may not be able to discern the fine structure of a radiant possible with the image forming extension to the transform technique, this technique is complementary to such analysis in that related radiant structure is easily discernible.

Similarly, the use of meteoroid speeds as an additional discriminant in radiant identification can be employed to great effect. The application of the Fresnel phase time technique to determine meteoroid speed in the case of low PRF medium frequency echo data has been shown to be particularly effective.

Some areas for improvement of the chosen techniques have been noted in this discussion. The relative strength of the Orionids shower is classed as weak from the data analysed here. Increasing the echo rate and hence the number of shower meteors

will allow statistically significant features to be better identified. However, any rise in meteor numbers may also increase demand for more stringent, statistically based, selection procedures. Currently, line identification by "eye" and using *a priori* radiant information is appropriate and straightforward to apply. However identifying previously unrecognised stream structure in high count rate data is more demanding and may require alternate methods of radiant identification (e.g. *Jones* [1977]).

Accompanying any enhancement of the line selection technique should be an increase in accuracy of the input parameters. *Jones & Morton* [1977] have noted that the sensitivity of the method is limited by the accuracy of the directional measurements. This is further discussed in future work section of Chapter 8.

Chapter 8

Conclusion

8.1 Summary

Overview

This thesis describes the refurbishment of the 2 MHz Buckland Park MF Doppler radar in order to examine its potential as a meteor radar while maintaining its capability as a general facility for atmospheric research; the subsequent application to meteor observations is also presented and discussed.

This entire refurbishment was motivated from the view point that successful , atmospheric and meteor research can only be conducted with equipment of specified and stable performance. The system was first thoroughly investigated for operational and design faults that had hitherto limited its performance. The antenna array, transmitter, receiver and computer control sub-systems were evaluated and the faults isolated were addressed. New equipment was developed and integrated into the system, and preventative maintenance programmes instituted. At the conclusion of these procedures verification of performance of each sub-system was undertaken and found to be within specification. Suggestions for future work on the equipment were also detailed.

In utilising the refurbished radar system for meteor observations, various experimental configurations were investigated. On 22 October 2000 the Orionids shower was successfully identified and the speeds of the meteoroids obtained using the Fresnel

phase time technique. Possible directions for future radar meteor work at MF are discussed.

Antenna array

Chapter 3 directed attention toward the performance and repair of the antenna array. This array is approximately 1 km wide, comprises 178 dipoles (89 crossed dipoles) and about 70 km of protected, exposed or buried coaxial cable. A mix of new and old infrastructure is a characteristic of this system, with relatively new cable used in conjunction with that installed in the late 1960's. The existing operational capability of the array was determined and found to be well below specification.

Time domain reflectometry (TDR) was the primary tool used to evaluate the performance of the array. Two TDR systems were discussed. The first a low resolution system for general cable-balun-antenna diagnosis and the second, a higher resolution system for specific cable fault location work.

Most faults uncovered in the cable-balun-antenna systems were confined to the cable sections, with water ingress being the dominant symptom. Balun associated faults were the next significant concern followed by the less significant antenna faults. Fault repair was prioritised and addressed in a coordinated programme of work.

After maintenance procedures the cable-balun-antenna (CBA) sub-systems examined were classified as "operational" or "operational with some minor fault". Only 11% were not operational due to serious faults. Appropriate techniques to address these more serious faults were proposed. Cable lengths were estimated using the TDR technique and found to be in good agreement with theoretically calculated lengths, thus providing a sound method of cable performance evaluation.

Cable system phase values derived using the atmospheric partial reflection array calibration technique were also evaluated as a diagnostic tool for cable water ingress. Results indicate this is a promising technique.

Results of the survey enabled projections to be made of likely future problems concerning the array and thus allow development of strategies to limit their occurrence

or effect. This involves an ongoing, scheduled, array monitoring and maintenance programme. A database of TDR profiles of each CBA system examined was established which can provide much needed data on specific CBA sub-systems as the array evolves over time.

Equipment

Chapter 2 focused attention on the radar transmitter and receiver sub-systems. Much attention was necessarily directed toward the operational behaviour of the three transmitter units. This transmitter system was found to be performing outside specification with the major consequence being the transmitted beam deviated markedly from that modelled. In addition to this, steering of the transmitted beam was ineffectual.

Problems were found to span most primary modules of the transmitter system. The power and phasing problems of all transmitters were found to be partly the result of extensive faults in the phase control modules, and solutions appropriate to each identified fault were implemented. A calibration method for these phase control modules was developed and successfully applied to the system. Further improvements in channel phasing were made with the re-tuning of the filter/TR switches and identification of an under-rated (choke) component across all transmitter chassis.

Significant failure of the power transistors on the 5.0 kW PA modules of transmitter unit three, possibly due to their implementation out of specification, was identified.

Beam steering function was restored to the two 25 kW transmitters via the identification of a manufacturing fault on one phase control module board. The third (50 kW) transmitter was then integrated into the system. This integration process revealed significant deficiencies in the transmitter's control system, including a non-standard design and manufacturing faults. These faults were rectified. The result of all this work is that beam steering operation was restored and verified.

With all common faults eradicated from the individual transmitter units, their operation side-by-side revealed a significant transmitter pulse leakage problem in transmitter unit three. A low frequency signal produced by this transmitter unit contaminated all data collected by the receivers connected to it. This spurious signal was found to be a characteristic inherent in the design of the 5.0 kW PA modules. Various solutions were proposed and evaluated, with the most effective approach determined to be the inclusion of a removable circuit that clips the transmitted pulse of the unwanted signal.

The behaviour of two types of receiver in the radar data acquisition system were compared and found to be significantly different in terms of their gain characteristics. This was not corrected but it is envisaged that minor adjustments could be made to the most recent design to standardise receiver behaviour. This, together with the re-implementation of the automatic gain control function and adjustment of the gain control algorithm, will further optimise radar performance for atmospheric observations. Other areas that were noted but not corrected included: a) measurable cross-talk confirmed to occur between the filter/TR switches which has some impact on the quality of signal recorded at the receivers and, b) data transfer problems between the RDAS and controlling PC which were apparent when the system was applied to meteor observations.

Following the optimisation of the existing radar system, new hardware was designed, constructed and evaluated. This was in the form of a power combining system and its genesis was detailed in Chapter 4. The design and layout of this equipment focused on future expansion, such as scaling to higher frequencies of operation if required. Facilities for adjustment of the transformer's characteristics were provided so as to enable connection to different antenna systems. This power combiner system resulted in a significant increase in power to a single or small groups of dipoles (or any antenna system for that matter).

Radar meteor data and reduction methods

Chapter 5 summarised the theoretical aspects under-pinning radar observations of the atmosphere and more specifically, meteor observations. From the radar meteor echo a wide variety of parameters can be deduced. These include the meteoroid mass, speed, deceleration, degree of fragmentation, and height of ablation; with 3 appropriately spaced radar sites the direction cosines of the trail and hence orbit of the meteoroid can be determined.

It has been shown that the 2 MHz radar meteor echoes give quantitative information on the height of ablation of the meteoroid, the amplitude-time and phase-time behaviour of the echo, the duration of the echo, and the position of the reflection point which is also the orthogonal point on the trail with respect to the radar site. Using this basic information specific techniques were evaluated to determine what parameters of those listed above could be derived from the 2 MHz data.

The most appropriate techniques were outlined in Chapter 6. Meteor angle-of-arrival was ascertained by a twin baseline interferometer using a non-optimal inter-element spacing dictated by the established array structure. Radar system phase errors were estimated via atmospheric partial reflection. These estimates were found to be relatively stable over extended time periods, but diurnal variations were apparent. The influence of mutual coupling effects on AoA results were also discussed.

Particular attention was given to possible techniques for determining meteoroid speed or velocity. The Fresnel phase time technique was deemed to be most suitable in this situation due to medium frequency radar studies of meteors requiring a relatively low PRF. The successful application of this technique to the data was described.

In order to detect shower meteors the optimal radar configuration was explored. To examine the direction of arrival data for the presence of meteor showers an established coordinate transform technique to determine the meteor radiant was selected amongst other similar techniques due to its efficacy in dealing with data exhibiting low hourly meteor count rates, characteristic of MF radars.

The development of suitable software for effective analysis of the data was discussed in the context of available software. Multi-channel MF radar data can place high demands on analysis software and a specific technique for handling large data sets was outlined.

Results

Extensive observations of shower and sporadic meteors were carried out and from the data set the period of the Orionids shower of 22 October 2000 was selected for particular study. To observe this shower, the radar was configured to optimise transverse radar echoes and track the source radiant through the early morning hours. A total of 108 meteor echoes were identified. The application of the coordinate transform technique of *Elford* [1954] to the direction of arrival data allowed identification of two groups of Orionid meteors contained within the shower event. The Orionids-Primary group contained 30 potential shower meteors with radiant coordinates $(\alpha,\delta)=(95°,16°)$. This radiant is in agreement with the radiant determined by other observational techniques. The Orionids-Secondary group contained 15 potential meteor echoes at radiant coordinates $(93.5°,21.0°)$. The meteoroid speed calculated by the Fresnel phase time technique was used as an additional discriminant. Assuming a shower speed near $60 \, \text{km s}^{-1}$, Orionids echoes were further isolated from low speed sporadic echoes within the potential echoes of each group. This resulted in 24 Orionids-P and 11 Orionids-S echoes being identified. The shower strength index of the Orionids observed over this period is thus ∼48%.

The sporadic meteor component was also examined over the same observation period. A peak in the sporadic speed distributions near 40-45 km s^{-1} was found. This is significantly higher than the expected sporadic speed of the helion/anti-helion meteoroid source and is attributed to a selection bias towards higher speed meteoroids inherent in radar observations.

The technique of *Elford* [1954] also allowed the identification of other structure in the reflection point distribution of 22 October 2000. However this structure exhibited

little coherence in height, speed etc. and it was concluded that no other showers were present at this time.

8.2 Conclusion

Within the constraints inherent in detecting and exploiting radar meteor echoes at MF, a successful outcome to the project as originally envisaged was achieved. However, the final result required a very extensive refurbishment of the 2 MHz radar research facility at Buckland Park, South Australia, and a major part of this project was devoted to this upgrade.

The basis of this project was the fact that radar observations at HF and at VHF have a height ceiling of about 110 km, although theoretical and optical studies indicate that a substantial fraction of meteor trails occur at heights up to 140 km. Previous observations at 2 MHz have shown that radar echoes can be detected up to this height. Thus the detection and study of radar meteor echoes at 2 MHz has the potential to study the meteoroid population that ablates at heights above 110 km and possibly to use Doppler studies of the trails to measure atmospheric winds at heights up to 140 km.

To set the project in context it needs to be emphasised that, in comparison to meteor observations at HF or VHF, there are significant detection issues at MF that do not arise at higher operating frequencies. These include the ambient radio noise, ionospheric scatter, and enhanced duration of the meteor echo. At a frequency of 2 MHz the observations are limited to times when the E-region echo is absent which restricts the period of observation to about 6-8 hours before sunrise. Further, to inhibit interference from the F-region echoes the PRF must be significantly below 100 Hz.

Following very substantial refurbishment of all parts of the radar system the facility was brought to near 100% operational status. The only current deficiency affecting this capability is the un-serviceability of a small percentage of the buried cable, but due to the large size of the array and the redundancy therein, the un-serviceable part

can be avoided while using the facility.

The near 100% result was achieved by focusing attention on each primary radar sub-system in turn, in an effort to address the high number of widely distributed system faults. Dividing a complex radar system into smaller, more manageable sub-systems reduced the number of problems faced at one time, reduced fault complexity and allowed each system to be fully optimised independent of the others. Such an approach is applicable to, and recommended for, other radar systems.

A further objective of standardising sub-system modules, such as the phase control, power amplifier and filter/TR switch modules, was successfully implemented and provides for both increased service-ability and reduced maintenance times.

It is considered that this current level of operational status achieved can be maintained. Organised monitoring, scheduled maintenance and regular system verification are the most effective approaches to facilitate this aim. This is aided in this case by the development and documentation of appropriate maintenance procedures specific to the MF Doppler radar (see *Woithe & Grant* [1999]). The scientific benefits of such an approach are numerous. Continuous observation of the atmosphere and repeatability of experiments is possible, and the radar is more easily adapted to new applications. Also there is more efficient use of supporting resources such as labour and test equipment which is of paramount importance when dealing with a system of large physical size, as in the case here.

Specific attention was devoted to the antenna array sub-system. A spatial analysis of the distribution of water ingress throughout the array identified the over-representation of the south east quadrant of the array in the data. This suggested that previous maintenance procedures to eradicate water from the air-cored dielectric, now thought to have happened through poorly sealed components in the original balun feed system, were inadequate. If indeed this is the case, the successful 1992/94 upgrading of balun and partial cable components to deter water ingress, coupled with the now more rigorous compressed air water eradication techniques, suggests future water ingress problems should be much less common and of a less severe nature than

that uncovered and addressed in this survey.

A fully functioning and optimised radar system is the ideal candidate for calibration. Various calibration techniques were discussed and if completed will allow more complete comparisons with data from other similarly calibrated radar sites.

Single site VHF meteor observations typically have determined meteoroid speeds and source radiants in addition to the more common parameters of angle-of-arrival, height, etc. However there has been a slower application of meteoroid speed techniques to the lower radar frequencies as many VHF techniques are not applicable in this situation. However the Fresnel phase time technique is well suited to the determination of MF meteoroid speeds in the solar bound range, and this study details the first known determination of meteoroid speed at radar frequencies as low as 1.98 MHz. Similarly, the coordinate transform technique of *Elford* [1954] is able to isolate weak shower activity from the sometimes overwhelming sporadic events from data acquired at this frequency.

The refurbishment of the radar system, together with application of appropriate data analysis techniques, has enabled the successful observations of the Orionids at medium frequency. Specifically, the identification of two Orionid radiant groups, separated by a declination of 5° within the Orionids shower is a significant finding. This reinforces the concept of a filamentary stream which presents differently on each encounter. Evidence supporting this characteristic of the Orionid stream has been gathered at other radar frequencies. As noted previously, *Jones* [1983] observed large fluctuations in Orionids declination from day to day, suggesting that it could be the result of transient burst of activity from filaments within the total stream. When developing a revised model of the Comet Halley meteor stream to incorporate recent observations, *McIntosh & Hajduk* [1983] noted that previous models had difficulties explaining changes in the position of maximum activity, which suggests a filamentary structure of the stream. Recently, preliminary observations of the Orionids at 54.1 MHz by *Badger* [2002] identified a wide variation in meteor echo hourly rate present in one of three fixed beam directions on 22 October 1999. This particular

beam direction was perpendicular to the Orionids radiant for some time, thus ensuring a high number of shower echoes, and suggests that the stream is arriving as "clumps" of particles.

As has been established previously, the Orionids shower is a result of the Earth's annual encounter with part of the stream of Comet 1P/Halley. The η-Aquarids shower in May is a result of another encounter with this stream and we might expect that results reported in this study may be observed in observations of this "sister" shower. Observations during 1998, 1999 and 2000 of the η-Aquarids at the Buckland Park site at 54.1 MHz displayed multiple activity peaks indicating the shower is produced by at least four distinct "filaments" [*Badger*, 2002].

These radar results are in contrast to a recent study of visual, photographic and video studies of the Orionids, where *Lindblad & Porubcan* [1999] suggest there is no substantial evidence for a very complicated radiant structure. It is important to note that the current radar observations focus on a smaller mass component of the Orionid stream which may in fact exhibit slightly different behaviour to that probed via visual observations. This places the current study in the context of probing a specific component of the Orionid stream complex.

The successful implementation of speed determination and the unparalleled height coverage offered at this low radar frequency has resulted in the detection of a few sporadic high height, low speed meteoroids. This suggests the benefit of a more comprehensive study of the sporadic meteoroid complex in order to isolate or identify meteoroids of distinctly different compositions, as suggested by *Elford* [2001*a*]. Sporadic (and shower) meteor observations may now be carried out routinely with the Buckland Park 2 MHz radar.

Medium frequency probing of the meteor height range presents challenging problems in itself. The dynamic nature of the ionosphere dictates that most successful radar meteor observations occur during quiet ionospheric conditions. Techniques to limit the effect of more common ionospheric phenomena on meteor observations have been outlined and may go some way to enabling near-continuous night-time meteor

observations at these frequencies. The prospect of continuous observations at these frequencies has benefits more far reaching than in terms of meteor research itself. Continuous meteor derived winds will enable an extension of the height range of the wind fields determined by other methods.

8.3 Future work

Recommendations for future work pertinent to each area of the radar system (i.e. transmitter/receiver hardware, antenna array, power combining system) were thoroughly discussed at the end of each respective chapter.

The discussion that follows details future work applicable to the Orionids data analysis outlined in Chapter 7 and then to meteor observations in general using the Buckland Park MF Doppler radar. The latter aspect of this discussion is organised in terms of hardware, software and future projects.

Because of the extended nature of the Orionids shower activity the analysis of data from consecutive days around the activity peak would be of considerable benefit[1]. This would facilitate 1) the isolation and hence estimation of the radiant and 2) establish the temporal behaviour of this or other radiants. If such data were analysed and the data combined, this would effectively increase the total meteor count rate to aid subsequent analysis. This has direct implications for obtaining more accurate mean shower parameters (i.e. height, speed etc.) as well as in the identification of weak showers (i.e. recognised or currently un-recognised showers). In addition to this a small increase in count rate may be possible if ambiguity can be removed from ambiguous echo angle-of-arrival estimates.

The successful observation of this shower is a consequence primarily of a reasonable ratio of shower to sporadic meteors, a moderate to high (and thus separable) shower speed and favourable ionospheric conditions. The first two factors mentioned here are expected to be repeated at any future observation date of this shower, while the

---

[1]The mains power supply to the radar system was interrupted during the observation period preventing analysis of contiguous daily observations in the current study.

likelihood of observing in favourable ionospheric conditions in the future is reasonable given October precedes the less favourable summer months. Provided observations are not taken during sunspot maximum, the prospects of further successful observations of the Orionids at MF are therefore good. Each of these factors applies equally well to the η-Aquarids sister shower in May. Here, the benefit of near winter observations may extend the observation period and increase the expected echo rate. In any case a more complete study of the meteoroid streams associated with Comet 1P/Halley is possible at medium radar frequencies, which has the potential to provide a different perspective on this not extensively studied stream.

While the flexibility of the Buckland Park MF radar system allows a wide variety of atmospheric investigation to be initiated, it is apparent that the system was not designed specifically for meteor observations. This is not a major concern however, given that some modification to the radar configuration and minor hardware improvements could significantly improve meteor observations and atmospheric observations in general. These improvements are discussed in the following paragraphs.

Given the atmospheric entry geometry of meteoroids, the implementation of a donut-like radiation pattern on transmission, similar to that modelled by *Nakamura et al.* [1991], would place maximum power at the zenith angles most likely to yield meteor echoes. However, this particular configuration is more suited to sporadic meteor observations than shower observations. Such an arrangement is possible given the available radar hardware and controlling software and could be implemented in alternation with a more conventional beam configuration for non-meteor data collection. In addition to this, the commissioning of the third (50 kW) transmitter, and designs for a pulse leakage circuit modification to limit the spurious signal inherent in its power amplifier modules, could see this unit integrated into the existing system for a substantial increase in transmitted power. Given suitable ionospheric conditions this could facilitate the detection of fainter meteors and increase the SNR of those already detected. Increasing the SNR of echoes would benefit meteor parameter reduction as

a not insignificant number of meteors echoes failed to produce vital parameters in this study due to poor echo SNR.

Ionospheric absorption can be significantly reduced by the use of right-hand circularly polarised (Ordinary or O-mode) transmit radiation. In this study, linearly polarised radiation was transmitted which suffers splitting at height of $\sim$100 km into O & E-modes, of which the Extra-ordinary mode (E-mode) is significantly absorbed and/or retarded. This is complicated by the fact that horizontal crossed dipoles fed in quadrature will only ensure circular polarisation close to the zenith [*Ceplecha et al.*, 1998], which has significant implications for the radiation produced at moderate off-zenith angles by steered pencil or donut-like beams. Similarly, reception of circularly polarised radiation must also be catered to. This has the advantage of limiting the effects of astigmatism in the receiving system and then shifts any further improvement in this regard to the less beneficial improvements in the antenna ground plane.

The use of O & E mode radiation has deeper implications for meteor work in that the full theoretical treatment of electromagnetic scattering from a meteor trail is polarisation dependent and thus future research will more closely compare experimentally obtained meteor echoes to theoretically modelled situations including these polarisation effects. This places some significance on the knowledge of polarisation of the radiation transmitted and received.

At a more practical level, significant improvements in the configuration of the interferometer used for reception is warranted. In the study described here, antennas used for reception were of orthogonal polarisation to those used for transmission. This was the only configuration available at the time of data collection and may have had the effect of reducing meteor echo rate observed. Future experiments should use the same polarisation antennas for reception as those used for transmission. To increase the signal at the receivers, the complete interferometer should be repositioned near the array centre, to reduce the effect of lengthy cable runs. Alternatively, a new interferometer could be constructed near the array centre to provide the optimal spacing of multiple half wavelengths so as to reduce mutual coupling effects. Interferometer

calibration techniques that omit the use of the atmospheric partial reflections should be implemented. In addition to this, the connection of single antennas to individual receivers may benefit from a transmit/receive switch to isolate the recorded signal from the transmit pulse and other effects. Obtaining a better impedance match to the receiver, than that achieved at present, is likely to increase the power detected by the receiver also.

The implementation of a solution to increase the data transfer rates from the radar controller to analysis computer will see a dramatic increase in total data collected over a similar observation period and thus a corresponding increase in total meteor echoes detected. This may be further optimised by increasing the length of time series collected to limit the number of echoes segmented at medium frequencies. Higher count rates translate directly to a better statistical analysis and to a greater understanding of the physical phenomenon under investigation. The facilitation of these improvements requires a thorough investigation of the RDAS and may ultimately demand a migration of the radar controller software from MS-DOS based to a Real Time Linux implementation.

The current radar experiment configuration software (radarcfg), can schedule multiple different experiments to occur during a set observation period. In terms of meteor observations, a data base of known major showers could be provided in order to direct a narrow beam to the optimum angle for individual shower observations as they occur each year. Such an arrangement is suggested as an alternate approach to the implementation of a donut-like beam as described above.

Of significant research and practical value is the simultaneous or near-simultaneous observation of meteors and other atmospheric phenomena. For instance the estimation of wind field behaviour or electron density from meteor echoes in comparison, or in complement to, that obtained from Full Correlation Analysis (FCA) or Differential Absorption Electron (DAE) concentration analysis is possible at the present time with some minor hardware alterations. These types of analyses generally require different transmit beam configurations coupled to individual receiving configurations. This

may be achieved by software selection of the appropriate transmit beam for a given antenna configuration and the consolidation of current receiver antenna configurations. Alternatively, the Time Domain Interferometry (TDI) technique does not require a vertically directed beam to ascertain winds and so may be integrated more easily with meteor observations of the type described in this study.

In terms of the software used, an automated detection algorithm should be implemented on the basis of knowledge gained from the manual detection procedures currently used. Also, the viability of transferring existing meteor analysis software to an "object orientated" approach seems to offer future benefits. Treating a meteor event as an individual object, with individual characteristics and requirements seems to be a more natural and flexible approach to dealing with this dynamic physical phenomenon than that offered via a "structured" programming approach.

Once optimised for meteor observations, the system could be applied to new research in this area. In this regard a unique opportunity exists with the current co-location of three meteor echo capable radars at the Buckland Park site. Multi-frequency observations (at 1.98 MHz, 31.0 MHz and 54.1 MHz) of meteor phenomena enable comprehensive testing of current meteor theory in an unprecedented fashion. At the forefront of questions to be answered is the true height distribution, often unobtainable due to the radar carrier frequency determined height ceiling affecting VHF radars. Radar meteor height response could then be better calibrated from a statistical analysis of multi-frequency observations of sporadic or shower events. This type of analysis could be applied to the many other meteoroid characteristics derived from radar data. Similarly, evaluation of the specific analysis techniques on common data at different frequencies is of value. For instance a direct comparison of the capability of the Fresnel phase time or Fresnel Transform technique to determine meteoroid speed could be undertaken on observations of the same shower. Alternatively, simultaneous multi-frequency observations of an *individual* meteor event would be of particular scientific interest. A similar type of comparison has been undertaken between VHF and

UHF resulting in 145 meteors observed by both systems and suggesting different scat-tering mechanisms are responsible for the echoes at each frequency [*Zhou et al.*, 1998]. Few multi-frequency studies, incorporating medium frequencies, have taken place to date and all have not had the opportunity to apply the Fresnel Transform technique which has the potential to probe the structure of these simultaneous echoes. While the infrastructure exists for such a study, a common timing reference would have to be established between each radar system, although timing accuracy would only need to be in the tens to hundreds of milliseconds range.

In terms of the work presented in this study, it was suggested when the radar system was first commissioned that the multi or dual frequency observation of meteors using a VHF radar operated during the day may be capable of isolating meteor events in the presence of strong ionospheric activity as seen by a 1.98 MHz radar [*Briggs & Elford*, 1968]. If attempted and successful, this has the potential to open up routine day-time MF meteor observations.

These multi-frequency studies may be further enhanced by utilising the MF radars inherent dual frequency design. As discussed previously, the antenna array and sections of the transmitter chassis are configured for operation at 5.94 MHz. The construction of additional equipment could see operation at this frequency and application to meteor study.

The comparison of meteor radar data with other meteoric or atmospheric obser-vational techniques is also suggested. For instance the use of a digital ionosonde co-located with the radar equipment offers numerous applications. As noted in sec-tions 1.2 and 6.1.1, modern digital ionosonde equipment is capable of meteor ob-servation in its own right. This is an alternate configuration to the simultaneous multi-frequency radar configurations suggested above. Moreover, standard ionosondes maybe best utilised in their designed role, that of near real-time analysis of the iono-sphere in terms of radio frequency propagation. This information can be applied as frequency management advice for the 1.98 MHz radar in order to choose the optimal operating times for meteor observations, or can provide a comprehensive picture of

the environment in which the radar has operated in - post data collection. This can aid in estimation of ionospheric absorption, signal retardation and layer structure contributing to range aliasing[2]. Comparison of radar data with visual, camera or video observations is also of value. Estimation of meteor heights can be compared, with a view to validating the radar derived heights at MF. Using *different* techniques to view the same phenomenon is perhaps closer to the ideal observation of a complete meteor event [*Ceplecha et al.*, 1998].

Also of interest is the relationship of the meteoroid flux on the Earth's atmosphere and the formation of sporadic-E layers and other ion layering phenomenon (see e.g. *Mathews* [1987]; *McNeil et al.* [2001]). MF radars are well positioned to examine this relationship given the height capabilities of this radar frequency and the variety of analyses that can be applied to such data.

As discussed in section 5.2.2, recent theoretical research into the effects of the geomagnetic field on meteor echoes predicts enhancements in echo duration depending on orientation of the radar beam and magnetic field. For the current system, maximum enhancements occur with a radar beam at 67° off-zenith. While the established beam polar pattern rapidly deteriorates at these angles, significant radiation may be available to detect these enhanced meteor echoes.

While not selected as a speed technique to be applied in this study, the potential of the Fresnel Transform technique of *Elford* [2001*b*] for a more complete evaluation of meteoroid characteristics suggests future work should be directed towards applying this technique on MF radar data. Application of this technique at MF is currently limited by the coarse sample resolution and congestion of the ionospheric radio environment.

The pervasive height distribution of meteor echoes, as observed at MF, can be viewed as detrimental to non-meteor radar observations. The inherent characteristics of the meteor echo, of having a wide dynamic range and being transient in nature, serve to "contaminate" a variety of atmospheric analysis (e.g. *Lees* [1987]; *Jarrott*

---

[2]Simultaneous ionosonde and radar meteor observations have been recorded and are earmarked for future analysis.

et al. [1989]). An increased understanding of these meteor echoes will better facilitate the development of effective filtering or signal processing techniques to be applied to these data and such investigations should be initiated. The dual benefit possible here is an increase in the quality of non-meteor analysis together with an additional source of meteor events for dedicated meteoroid analysis.

Initially, the development of the power combining system described in this thesis was motivated partially for investigations into obtaining surface wind estimates from ocean sea-scatter. The transportable nature of the MF transmitter and receiver system makes it possible to locate this equipment at a coastal site, coupled to a surface wave generating antenna array via the power combining system, to further investigate this phenomenon. Atmospheric winds could also be obtained by switching to an array producing a vertically directed beam.